Article

Cell Metabolism

Global Analysis of Plasma Lipids Identifies Liver-Derived Acylcarnitines as a Fuel Source for Brown Fat Thermogenesis

Graphical Abstract

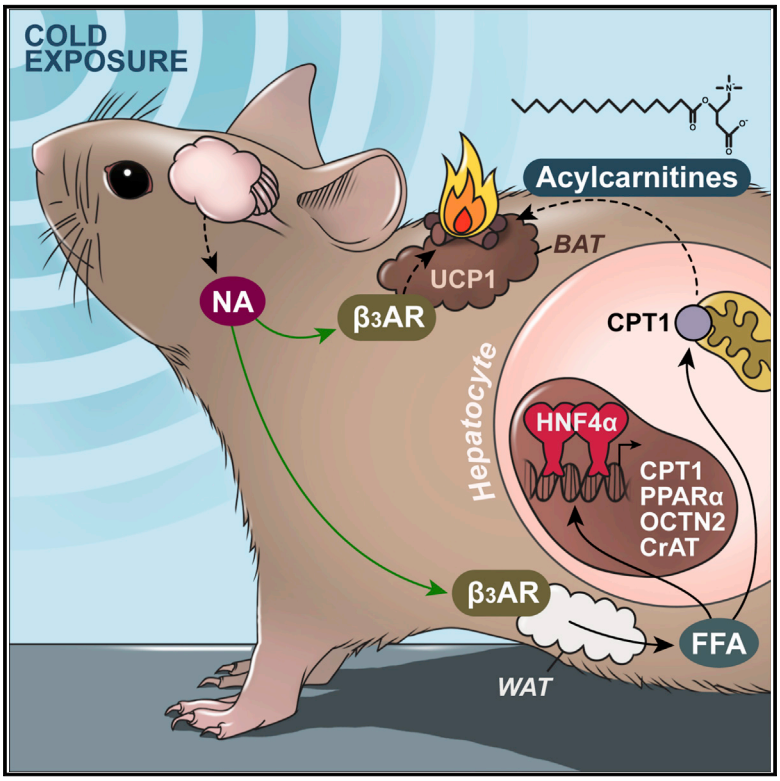

Authors

Judith Simcox, Gisela Geoghegan, John Alan Maschek, ..., Rudolf Zechner, James Cox, Claudio J. Villanueva

Correspondence

villanueva@biochem.utah.edu

In Brief

Simcox et al. identify acylcarnitines as a novel source of energy for brown fat thermogenesis in mice and show that in response to cold, the liver activates a transcriptional program through HNF4α to increase acylcarnitine production. Blocking hepatic acylcarnitine synthesis impairs adaptive thermogenesis.

Highlights

- Increase in plasma acylcarnitines is required for adaptive thermogenesis
- Adipose tissue lipolysis promotes hepatic acylcarnitine production
- HNF4α stimulates expression of genes involved in acylcarnitine metabolism
- Brown adipocytes increase uptake of acylcarnitines in response to the cold

Simcox et al., 2017, Cell Metabolism *26*, 509–522
September 5, 2017 © 2017 Elsevier Inc.
http://dx.doi.org/10.1016/j.cmet.2017.08.006

Cell Metabolism
Article

Global Analysis of Plasma Lipids Identifies Liver-Derived Acylcarnitines as a Fuel Source for Brown Fat Thermogenesis

Judith Simcox,[1] Gisela Geoghegan,[1] John Alan Maschek,[1] Claire L. Bensard,[1,8] Marzia Pasquali,[2,3] Ren Miao,[1] Sanghoon Lee,[1] Lei Jiang,[4] Ian Huck,[5] Erin E. Kershaw,[6] Anthony J. Donato,[7] Udayan Apte,[5] Nicola Longo,[2,3] Jared Rutter,[1,8] Renate Schreiber,[9] Rudolf Zechner,[9] James Cox,[1] and Claudio J. Villanueva[1,10,*]

[1]Department of Biochemistry
[2]Department of Pathology
[3]Department of Pediatrics
University of Utah School of Medicine, Salt Lake City, UT 84112, USA
[4]Children's Research Institute, University of Texas Southwestern Medical Center, Dallas, TX 75390, USA
[5]Department of Pharmacology, Toxicology, and Therapeutics, University of Kansas Medical Center, Kansas City, KS 66160, USA
[6]Department of Medicine, Division of Endocrinology and Metabolism, University of Pittsburgh, Pittsburgh, PA 15213, USA
[7]Department of Exercise and Sport Science, Geriatric Research, Education, and Clinical Center, Veteran's Affairs Medical Center, Salt Lake City, UT 84112, USA
[8]Howard Hughes Medical Institute, University of Utah School of Medicine, Salt Lake City, UT 84112, USA
[9]Institute of Molecular Biosciences, University of Graz, Heinrichstrasse 31, 8010 Graz, Austria
[10]Lead Contact
*Correspondence: villanueva@biochem.utah.edu
http://dx.doi.org/10.1016/j.cmet.2017.08.006

SUMMARY

Cold-induced thermogenesis is an energy-demanding process that protects endotherms against a reduction in ambient temperature. Using non-targeted liquid chromatography-mass spectrometry-based lipidomics, we identified elevated levels of plasma acylcarnitines in response to the cold. We found that the liver undergoes a metabolic switch to provide fuel for brown fat thermogenesis by producing acylcarnitines. Cold stimulates white adipocytes to release free fatty acids that activate the nuclear receptor HNF4α, which is required for acylcarnitine production in the liver and adaptive thermogenesis. Once in circulation, acylcarnitines are transported to brown adipose tissue, while uptake into white adipose tissue and liver is blocked. Finally, a bolus of L-carnitine or palmitoylcarnitine rescues the cold sensitivity seen with aging. Our data highlight an elegant mechanism whereby white adipose tissue provides long-chain fatty acids for hepatic carnitilation to generate plasma acylcarnitines as a fuel source for peripheral tissues in mice.

INTRODUCTION

Cellular metabolic networks evolved through the selective pressures of starvation and cold exposure, two energetically demanding conditions that require dynamic communication between tissues to maintain survival. During starvation, catecholamines signal to β-adrenergic receptors in the white adipose tissue (WAT) to mobilize lipid stores as free fatty acids (FFAs). Preferential use of circulating fatty acids by the liver and muscle during fasting preserves glucose stores for the brain. Throughout this metabolic switch, the liver uniquely provides ketones that can be metabolized by neurons in the CNS to generate ATP. This switch in primary fuel sources between tissues is regulated by metabolic substrate competition and inhibitory signaling in the Randle cycle (Hue and Taegtmeyer, 2009). In contrast to fasting, cold exposure stimulates energy expenditure, a consequence of fueling thermogenesis. During cold exposure, there is activation of the β3-adrenergic receptor (β3AR), leading to increased triglyceride lipolysis in white adipocytes and activation of thermogenesis in brown adipocytes (Lafontan and Berlan, 1993). However, little is known about the metabolic adaptations that occur in other cell types during acute cold challenge.

The brown adipose tissue (BAT) plays a major role in protecting against the cold through non-shivering thermogenesis. Brown adipocytes generate heat by disrupting ATP synthesis in the mitochondria through the uncoupling protein 1 (UCP1), which allows protons to flow across the inner mitochondrial membrane to release potential energy as heat (Cannon et al., 1982). Mice lacking UCP1 develop hypothermia with acute cold challenge; however these mice are able to adapt to the cold with incremental reduction in ambient temperature, suggesting that alternative mechanisms of thermogenesis are at play (Golozoubova et al., 2001). To replenish the proton gradient, brown adipocytes increase utilization of both glucose and fatty acids, generating additional heat as a byproduct of cellular metabolism (Seale et al., 2009). During cold exposure, the BAT initially relies on glucose, and when activated increases glucose uptake (Orava et al., 2011; Yu et al., 2002). In addition to carbohydrates, brown adipocytes utilize fatty acids from triglyceride-rich lipoproteins and FFAs released by white adipocytes (Bartelt et al., 2011; Chondronikola et al., 2014). Mice lacking adipose triglyceride lipase (ATGL) in adipocytes are unable to maintain their body temperature

during a cold challenge, highlighting the importance of energy mobilization for thermogenesis (Haemmerle et al., 2006). However, more research is needed to identify additional fuel sources, beyond glucose and FFAs, that drive thermogenesis.

Mitochondrial fatty acid oxidation in the liver is a tightly regulated process that is activated upon fasting. After entry into cells, long-chain fatty acids are activated by acyl-CoA synthetase and conjugated with carnitine by CPT1, the rate-limiting enzyme in long-chain fatty acid oxidation (Esser et al., 1993; Fingerhut et al., 2001; Longo et al., 2006; Schooneman et al., 2013). Carnitine is transported into cells through a cell-surface transporter, Octn2 (Slc22a5) (Tamai et al., 1998). Conjugation with carnitine allows the transport of fatty acids across the inner mitochondrial membrane through the carnitine-acylcarnitine translocase (CACT [Slc25a20]) (Ramsay et al., 2001). Once in the matrix, carnitine is removed, and fatty acids are destined for oxidation after activation by CPT2 to generate fatty acyl-CoAs (Gempel et al., 2002). CPT1 mRNA is regulated by the transcription factor HNF4α, a nuclear receptor that plays a key role in liver development and mitochondrial energetics (Martinez-Jimenez et al., 2010). Mutations in HNF4α lead to maturity-onset diabetes of the young type 1 (MODY 1), a disorder characterized by defective glucose-stimulated insulin secretion (Yamagata et al., 1996). During exercise and fasting, acylcarnitines are elevated in the plasma and are thought to reflect incomplete fatty acid oxidation (Schooneman et al., 2013). Acylcarnitines are also elevated in several inborn errors of metabolism, including disorders of fatty acid oxidation in which mutations in MCAD, VLCAD, and LCHAD can lead to death (Shekhawat et al., 2005). Although circulating acylcarnitine levels are elevated in various conditions of metabolic stress, very little is known about their role in systemic energy metabolism and their regulation.

In this study, we performed non-targeted lipidomics of plasma and found that long-chain acylcarnitines (LCACs) were induced in response to cold exposure or treatment with β3AR agonist CL-316,243. We hypothesized that acylcarnitines served a greater role than as a byproduct of fatty acid oxidation, but rather as a mechanism to provide fuel for thermogenesis. Knockdown studies targeting hepatic Cpt1a/b show a requirement for hepatic acylcarnitine synthesis for adaptive thermogenesis. These studies also led to a previously unappreciated role for hepatic HNF4α in regulating cold-induced changes in expression of enzymes involved in hepatic acylcarnitine metabolism. We demonstrate that this transcriptional program requires ATGL-mediated adipose tissue lipolysis of FFAs to activate HNF4α and serve as a substrate for acylcarnitine synthesis. With aging, mice show reduced plasma acylcarnitine levels in response to the cold and display a cold-sensitive phenotype. This can be reversed with carnitine or palmitoylcarnitine supplementation. Our findings suggest a novel role for the liver in thermogenesis, as well as uncover a well-orchestrated inter-tissue communication system to upregulate energy mobilization for heat production.

RESULTS

Global Lipid Analysis of Plasma from Mice Exposed to Cold and Identification of Acylcarnitines as a Cold-Induced Circulating Lipid

To understand the metabolic changes that occur during acute cold exposure, mice were placed in room temperature (24°C) or cold (4°C) for 5 hr, and plasma was analyzed using liquid chromatography-mass spectrometry (LC-MS)-based lipidomic analysis; lipids are displayed as a heatmap after cluster analysis using MetaboAnalyst 3.0 (Figure 1A). A total of 287 circulating lipids significantly changed ($p \leq 0.05$) in response to cold exposure, and 93 lipids were elevated, while 194 lipids were reduced. Further analysis and identification of the lipids or derivatives that were significantly ($p < 0.01$) upregulated by 2-fold showed a high representation of LCAC species (Figure 1B). We confirmed that these lipids were LCACs using LC-tandem MS (LC-MS/MS). To determine if the elevated LCACs reflected a change in thermogenic potential, we utilized aged mice as a physiologically relevant model of impaired thermogenesis. As mice and humans age, there is a loss of BAT function and increased sensitivity to hypothermia (Sellayah and Sikder, 2014; Yoneshiro et al., 2011). Therefore, we compared plasma lipidomic profiles between 3-month-old and 24-month-old mice and found a temperature-dependent divergence in the plasma lipid signature (Figure 1C), in which older mice have a blunted response in the cold. To test whether LCAC species were reduced in older mice, we measured 14:0-carnitine, 16:1-carnitine, 18:0-carnitine, and 18:2-carnitine levels in the plasma, and found that 14:0-carnitine was elevated 12-fold in response to the cold, compared with a modest increase of 2-fold in 24-month-old mice (Figure 1D). In our initial analysis, we only identified LCACs, and we were curious whether other acylcarnitine species were altered. Using ultra-performance LC-MS/MS (UPLC-MS/MS), we quantified many of the previously identified acylcarnitine species and found that the sum of short-chain acylcarnitines (SCACs) (C2–C5), medium-chain acylcarnitines (MCACs) (C6–C12), and LCACs (C14–C18) (Figures 1E and S1) was elevated in response to cold exposure, with the greatest increase in 3-month-old mice. Notably, older mice had higher basal levels of LCACs, MCACs, and SCACs at room temperature but a clear blunted response in the cold (Figure 1E). In contrast, plasma carnitine levels were reduced in response to the cold in both 3-month-old and 24-month-old mice (Figure 1E). These results are consistent with impaired thermogenesis seen in 24-month-old mice (Figures S1E and S1F) and suggest a loss of metabolic flexibility that impairs the response to energetically stressful stimulus.

Cold Exposure Stimulates Expression of Enzymes Involved in Acylcarnitine Metabolism in the Liver

Circulating acylcarnitine levels change during acute energetic stress, including exercise and fasting (Costa et al., 1999; Hiatt et al., 1989; Yamaguti et al., 1996). These acute changes are regulated in part by transcriptional changes in components of the carnitine shuttle (Song et al., 2010; Vila-Brau et al., 2013). To test which tissues were contributing to the increase in acylcarnitine levels, we measured the expression of genes involved in acylcarnitine metabolism in the liver, skeletal muscle, and BAT. In the liver, we found the expression of Cpt1b, Octn2, Cact, Cpt2, and CrAT was increased in response to cold exposure, while the expression of Bbox1, an enzyme involved in carnitine synthesis, was not altered (Figure 2A). Western blot analysis showed increased levels of Cpt1b; however, Cpt1a was unchanged when comparing livers from mice at 24°C and 4°C for 5 hr (Figure 2B). A longer cold exposure of 8 hr led to

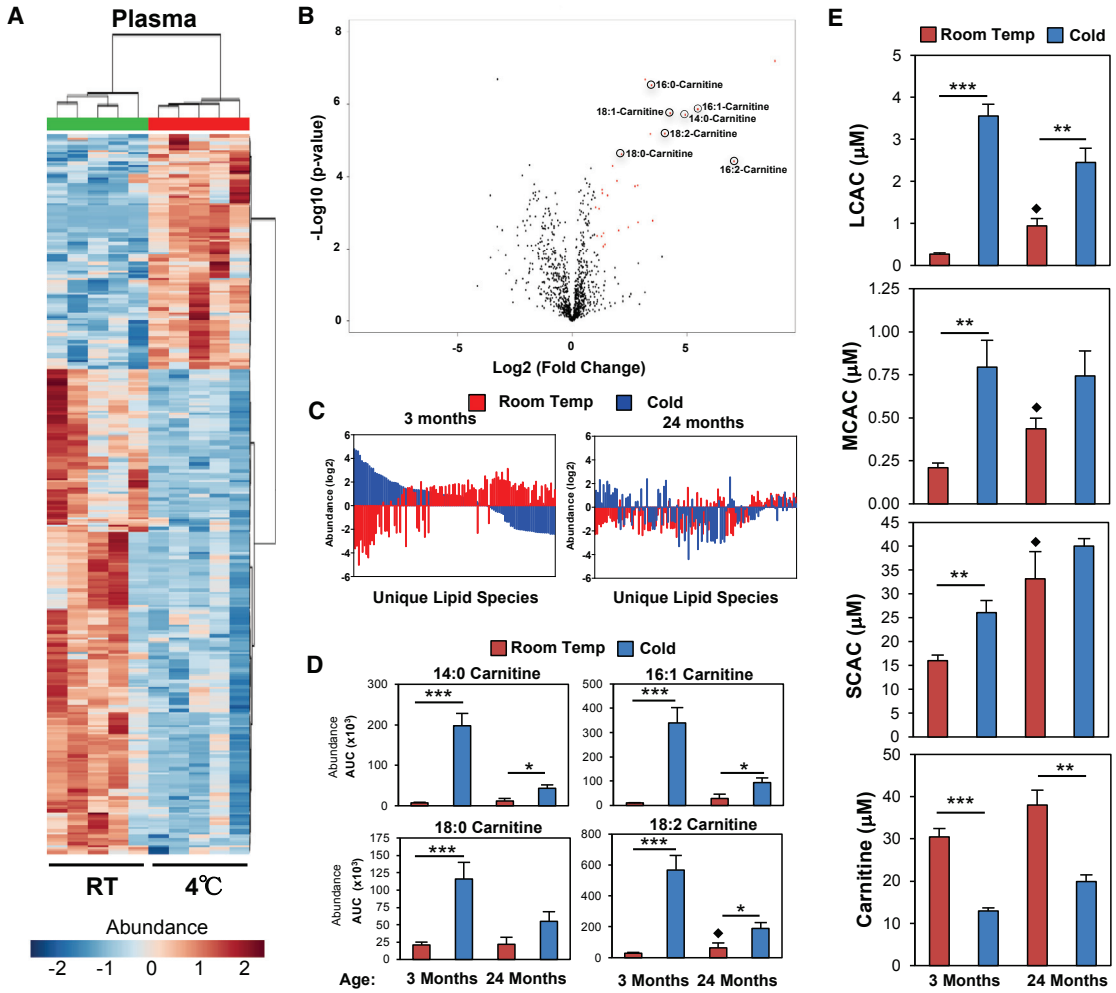

Figure 1. Acylcarnitine Levels in the Blood Are Elevated in Response to Cold Exposure

(A) Heatmap and cluster analysis of 281 lipids from plasma of 3-month-old C57BL6J male mice at room temperature (24°C) or cold (4°C). Samples were run on an Agilent 6490 LC-MS and analyzed using MetaboAnalyst 3.0. n = 5/group.

(B) Volcano plot of LC-MS-based lipidomics from the plasma of 3-month-old C57BL6J male mice at room temperature or cold. Lipids that are increased 2-fold in cold/room temperature and have a p value below 0.01 are labeled in red. Long-chain acylcarnitine species were identified through LC-MS/MS. n = 5/group.

(C) Significance analysis of microarray analysis of LC-MS lipidomics of plasma from room temperature versus cold in 3-month-old or 24-month-old C57BL6J male mice. n = 4–5/group.

(D) Plasma acylcarnitine levels of 3-month-old and 24-month-old C57BL6J male mice at room temperature or cold. n = 4–5/group.

(E) Plasma levels of long-chain acylcarnitine (LCAC), medium-chain acylcarnitines (MCACs), short-chain acylcarnitines (SCACs), and carnitine in the plasma of 3-month-old and 24-month-old C57BL6J male mice as measured by LC-MS. n = 4–5/group.

Data are presented as means ± SEM. *p ≤ 0.05, **p ≤ 0.01, ***p ≤ 0.001, room temperature versus cold. ◆p ≤ 0.05, 3 months versus 24 months room temperature. See also Figure S1.

detectable increases in Cpt1a, Cpt1b, and Octn2 (Figure 2B). Western blot analysis of livers from mice at 30°C and 4°C showed increases in Cpt1b and Octn2. In contrast, there were no detectable changes in gene expression of Cpt1b, Octn2, CrAT, and CACT in the skeletal muscle or BAT, except for increased expression of Octn2 (Figure S2A). To test whether the increase in circulating acylcarnitines was due to BAT, we measured acylcarnitines in UCP1-DTA mice that lack BAT (Lowell et al., 1993). In response to the cold, UCP1-DTA mice have a similar induction in acylcarnitines when compared with littermate controls (Figure S2B). Both 14:0-carnitine and 18:1-carnitine in the blood were elevated approximately 2-fold in response to a 4-hr cold exposure. Although the basal levels tend to be lower, the similar fold induction in control and mice lacking BAT suggests that the source of acylcarnitines is not brown adipocytes.

Targeting Acylcarnitine Synthesis through Knockdown of Hepatic Cpt1a and Cpt1b Lowers Both Serum Acylcarnitines and Core Body Temperature in the Cold

To test whether the liver was the source of acylcarnitines and to test their requirement for adaptive thermogenesis, we developed

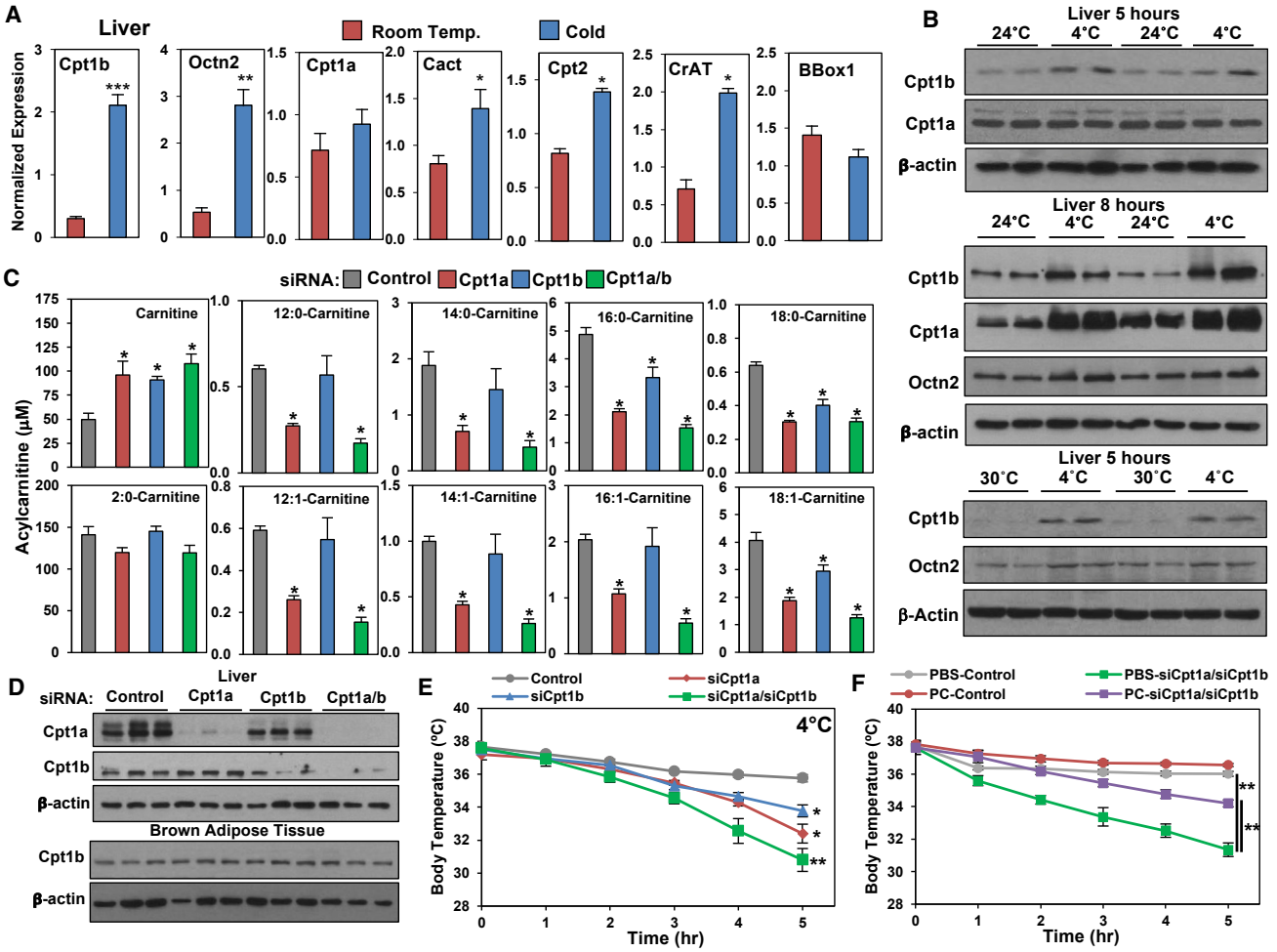

Figure 2. Cold Stimulates Expression of Genes Required for Acylcarnitine Metabolism, and Knockdown of Hepatic Cpt1 Leads to Cold Sensitivity

(A) Gene expression measured by real-time PCR in livers of 3-month-old C57BL6J male mice at room temperature (24°C) or cold (4°C) for 5 hr. n = 5/group.

(B) Western blot analysis of livers detecting Cpt1b, Cpt1a, Octn2, and β-actin. Three-month-old C57BL6J mice were exposed to room temperature or cold for 5 or 8 hr, as well as thermoneutrality (30°C) or cold (4°C) for 5 hr. n = 4/group.

(C) Serum long-chain acylcarnitine levels for 3-month-old C57BL6J mice at 4°C treated with liver-targeting liposomes containing siRNA to a scrambled control (Control), Cpt1a (siCpt1a), Cpt1b (siCpt1b), or a mixture of Cpt1a and Cpt1b (siCpt1a/siCpt1b) (n = 5/group).

(D) Western blots of liver and BAT of 3-month-old C57BL6J mice at 4°C treated with control siRNA, siCpt1a, siCpt1b, or siCpt1a/siCpt1b. Tissues were excised after 5 hr of cold exposure. n = 3/group.

(E) Cold tolerance test at 4°C of 3-month-old C57BL6J mice treated with control (siScramble), siCpt1a, siCpt1b, or siCpt1a/siCpt1b. n = 4–5/group.

(F) Cold tolerance test at 4°C of 3-month-old C57BL6J mice treated with control (siScramble) or siCpt1a/Cpt1b. Mice were given a single intravenous dose of PBS or palmitoylcarnitine. n = 5–6/group.

All transcripts were normalized to RPL13. Data are presented as means ± SEM. *p ≤ 0.05, **p ≤ 0.01, ***p ≤ 0.001. See also Figure S2.

small interfering RNAs (siRNAs) that target hepatic Cpt1a or Cpt1b (Figures 2D and S2C) using a liver *in vivo* transfection reagent (Bukong et al., 2014). Notably, siRNAs for both Cpt1a and Cpt1b reduced serum acylcarnitine levels, with the greatest effects seen when both Cpt1a and Cpt1b siRNAs were administered (Figure 2C). Knockdown of individual isoforms of Cpt1 resulted in reduced levels of several circulating acylcarnitines; siRNA targeting Cpt1a reduced all LCACs measured, while siRNA for Cpt1b only reduced 16:0, 18:0, and 18:1. Knockdown studies showed a direct effect on the liver, but knockdown was not observed in BAT or skeletal muscle (Figure S2D). Using western blot analysis, we found that Cpt1b, the major isoform in BAT, was not affected when Cpt1b siRNA was administered (Figure 2D). Histological analysis of livers of siRNA-treated mice showed similar morphology, suggesting lack of liver damage (Figure S2E), and found similar serum triglyceride levels between mice treated with scrambled siRNA or Cpt1a/Cpt1b siRNA (Figure S2F). To test whether liver-derived acylcarnitines are required for adaptive thermogenesis, we measured core body temperature hourly in the cold. We found that mice administered siRNAs targeting Cpt1a, Cpt1b, or both Cpt1a and Cpt1b had reduced core body temperature when compared with mice administered scrambled siRNAs (Figure 2E), in which the greatest drop in temperature was detected when both Cpt1a and

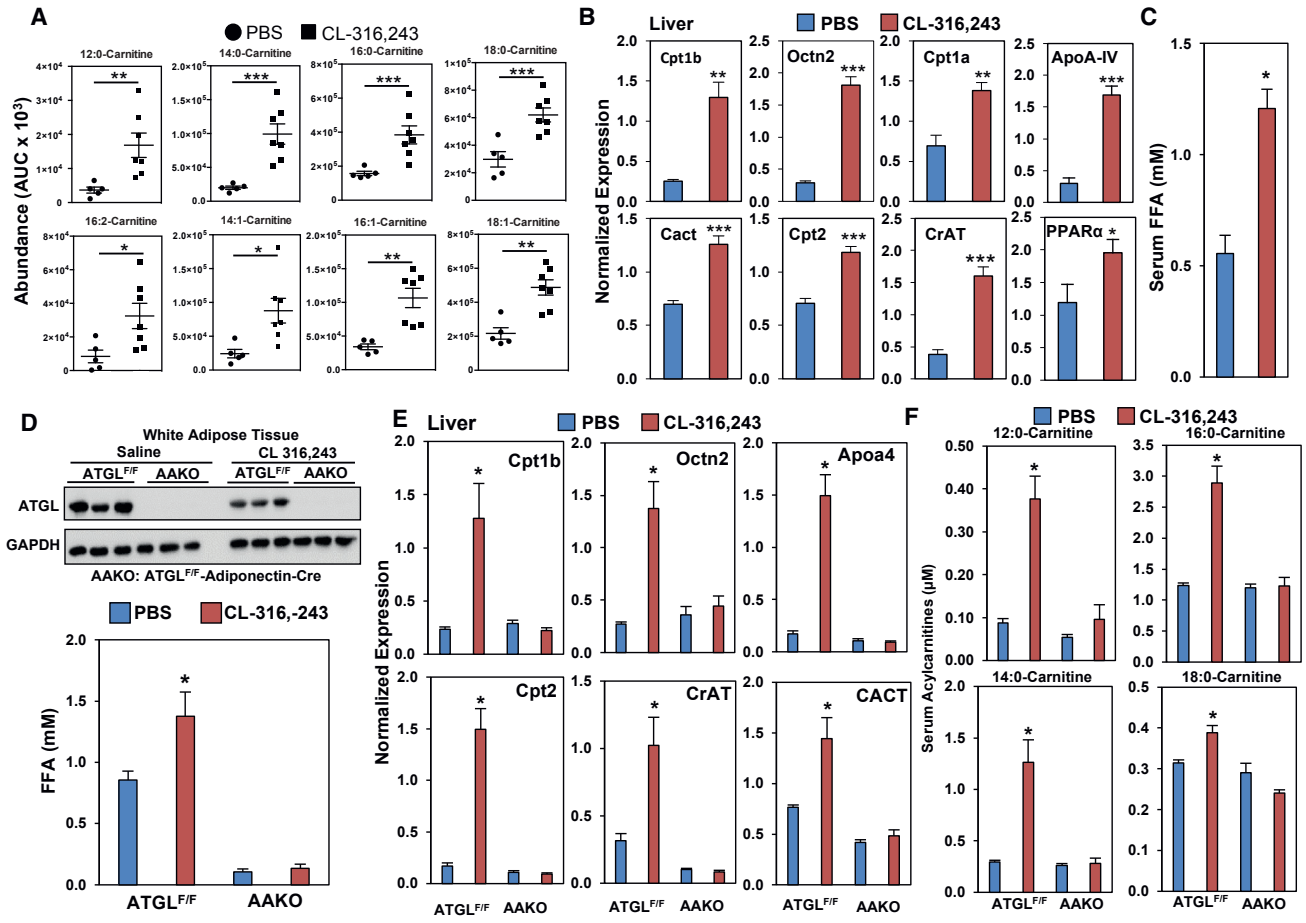

Figure 3. Adipose Tissue Lipolysis Promotes Acylcarnitine Production and Regulates Hepatic Gene Expression

(A) Serum acylcarnitine levels as measured by LC-MS in 3-month-old mice treated with PBS or CL-316,243. n = 5–7/group.

(B) Expression of genes involved in acylcarnitine and lipid metabolism in the liver of 3-month-old mice treated with PBS or CL-316,243. n = 5–7/group.

(C) Serum FFA level in mice treated with PBS or CL-316,243. n = 5–7/group.

(D) ATGL protein levels in the WAT and serum FFA levels of ATGL$^{F/F}$ and AAKO mice treated with PBS or CL-316,243. n = 5/group.

(E) Gene expression in the livers of ATGL$^{F/F}$ and AAKO mice treated with PBS or CL-316,243. n = 5/group.

(F) Serum acylcarnitine levels of ATGL$^{F/F}$ and AAKO mice treated with PBS or CL-316,243. n = 5/group.

All transcripts were normalized to RPL13; statistical analysis completed used two-way ANOVA. Data are presented as means ± SEM. *p ≤ 0.05, **p ≤ 0.01, ***p ≤ 0.001. See also Figure S3.

Cpt1b were knocked down. Simply reintroducing palmitoylcarnitine through the tail vein increased core body temperature in mice treated with siRNAs targeting Cpt1a and Cpt1b (Figure 2F).

Activation of Adipose Tissue Lipolysis Promotes Hepatic Gene Expression and Acylcarnitine Production

During cold exposure, body temperature is maintained through both shivering and non-shivering thermogenesis. There is evidence that exercise leads to elevated acylcarnitine levels; therefore, we hypothesized that shivering might trigger an induction in acylcarnitines as well. To rule out shivering, we used a stimulus of non-shivering thermogenesis through selective activation of β3AR using CL-316,243, which stimulates thermogenesis in brown adipocytes and lipolysis in white adipocytes. Mice were treated with CL-316,243 (Himms-Hagen et al., 1994) or vehicle control, and we found that CL-316,243 stimulates serum acylcarnitines, as noted by the elevated levels of 12:0-,14:0-,14:1-, 16:0-, 16:1-, 16:2-, 18:0-, 18:1-, and 18:2-carnitine when compared with controls (Figure 3A). In parallel, we measured the expression of genes involved in acylcarnitine metabolism and found increases in hepatic Cpt1b, Octn2, Cpt1a, Cact, Cpt2, and CrAT (Figure 3B). Notably, many of these transcripts are direct targets of HNF4α, including well-established targets such as PPARα and Apoa4, which were also induced by CL-316,243 (Figure 3B). HNF4α is a nuclear receptor that is activated by fatty acids. In BAT, we found increased expression of Octn2 and Cact, while Cpt2 and Acat1 were reduced, and Cd36, Cpt1b, Slc16a, and CrAT were unchanged (Figure S3A). CL-316,243 is a selective β3AR agonist, yet it was able to stimulate changes in hepatic gene expression despite the lack of β3AR expression in the liver. This observation and the increased expression of HNF4α targets led us to test whether FFAs released from the WAT in response to β3AR

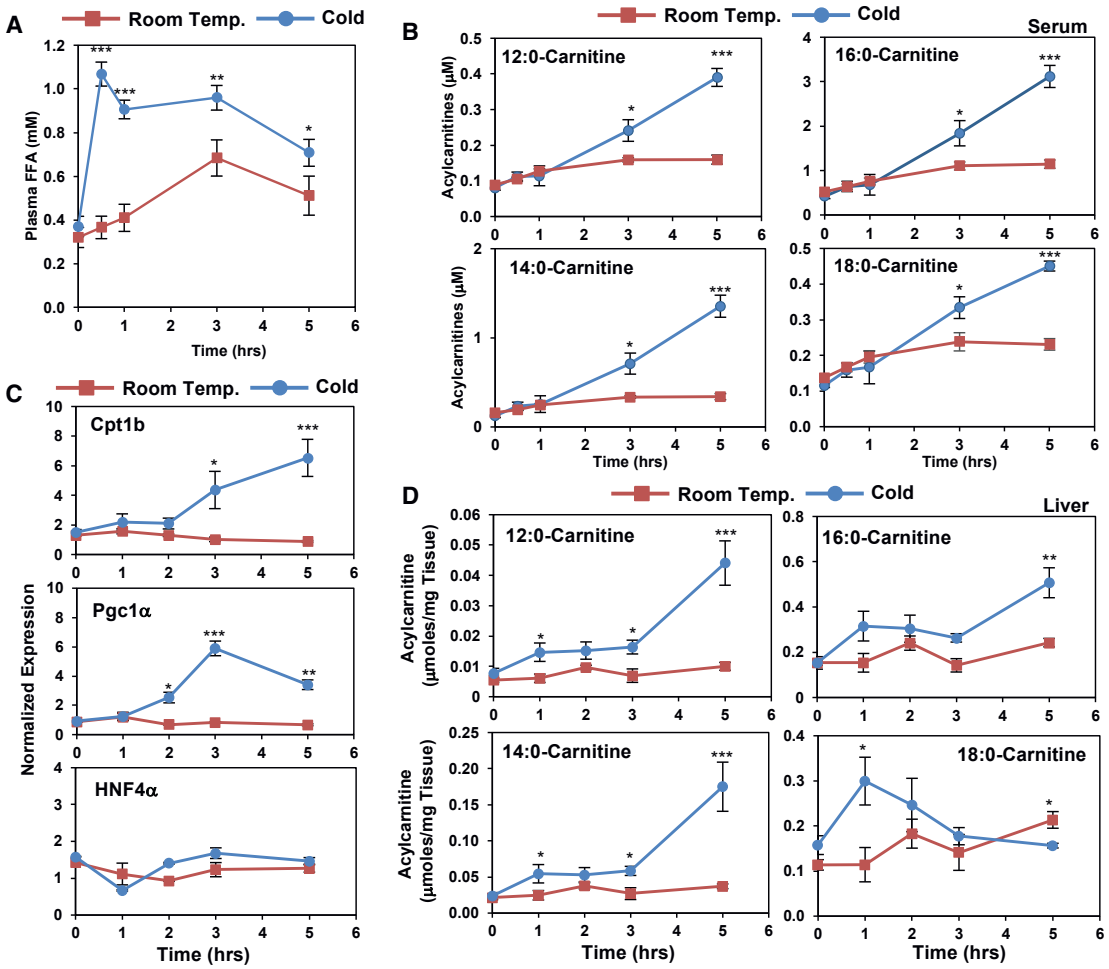

Figure 4. Time-Dependent Changes in Serum and Hepatic Acylcarnitines

(A) Time course of serum free fatty acid (FFA) and palmitoylcarnitine levels of 3-month-old male mice exposed to room temperature (24°C) or cold (4°C). n = 5/group.

(B) Time course of serum LCAC levels of 3-month-old C57BL6J mice placed in room temperature or cold. n = 5/group.

(C) Gene expression changes by real-time PCR analysis from livers of C57BL6J mice exposed to room temperature or cold. n = 5/group.

(D) Liver acylcarnitine levels measured by LC-MS from C57BL6J mice exposed to room temperature or cold. n = 5/group.

All transcripts were normalized to RPL13. Data are presented as means ± SEM. For comparison of room temperature versus 4°C, *$p \leq 0.05$, **$p \leq 0.01$, ***$p \leq 0.001$.

activation could be driving the transcriptional response in the liver (Figure 3C). To test whether adipose tissue lipolysis is required, we generated adipose-specific ATGL knockout (AAKO) mice and treated them with PBS or CL-316,243 (Figure 3D) (Schoiswohl et al., 2015). Compared with controls, AAKO mice were deficient in ATGL and had reduced FFA levels with PBS or CL-316,243 treatment (Figure 3D). Loss of ATGL in adipocytes blocked the induction in Cpt1b, CrAT, Octn2, Cpt2, ApoA4, and CACT in the liver, and blocked the increases in circulating LCACs (Figure 3F). To test the acute effects of inhibiting ATGL, we treated mice with ATGL inhibitor Atglistatin. Atglistatin treatment attenuated the cold-induced rise in circulating FFAs, which also led to impaired thermogenesis, and abolished the transcriptional changes in hepatic acylcarnitine transcripts and changes in circulating LCACs (Figures S3B–S3E).

Time-Dependent Changes in FFAs Precede Induction of Serum Acylcarnitines, Hepatic Gene Expression, and Liver Acylcarnitine Levels

The reliance of hepatic acylcarnitine production on changes in FFA release from the WAT suggests that FFAs may be acting as a substrate for LCAC production or as a signal to induce changes in hepatic gene expression. In either role, we predicted that changes in circulating FFAs would precede the cold-induced rise in serum LCACs. To test this idea, we performed a time course to understand the changes in FFAs, acylcarnitines, and hepatic gene expression. We found that FFAs increased to 1.1 mM within 30 min of cold exposure (Figure 4A), while increases in serum LCACs occur later, after 3 hr of cold exposure (Figure 4B). Transcript levels of hepatic Cpt1b exhibit a similar increase at 3 hr, which is preceded by the increased expression of PGC-1α, a strong transcriptional coactivator of HNF4α

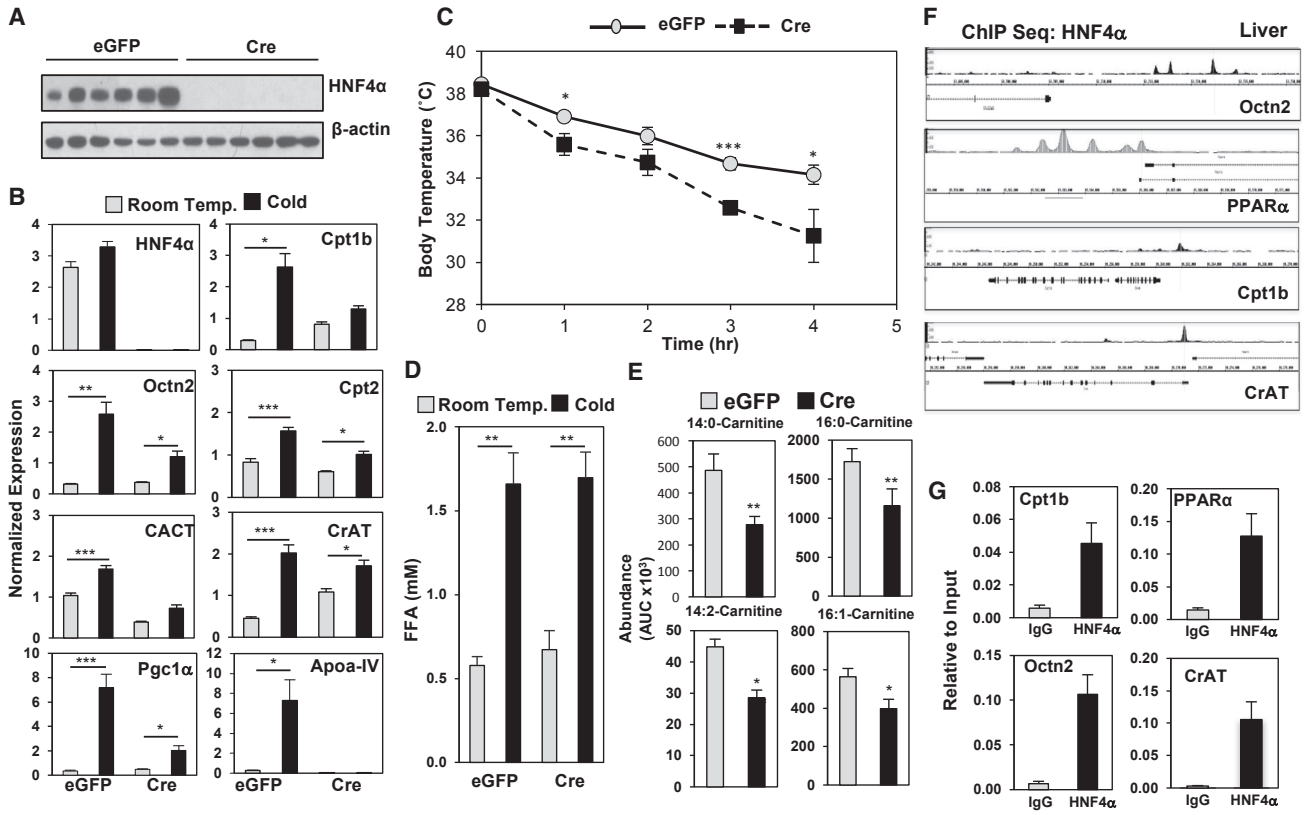

Figure 5. Hepatic HNF4α Regulates Acylcarnitine Metabolism in the Liver of Cold-Exposed Mice

(A) Western blot analysis of HNF4α and β-actin in the liver of HNF4α$^{F/F}$ mice infected with AAV8-TBG-eGFP (EGFP) or AAV8-TBG-eGFP-Cre (Cre). n = 6/group.

(B) Gene expression changes by real-time PCR analysis of livers from HNF4α$^{F/F}$ mice infected with EGFP or Cre. Mice were challenged with cold or room temperature for 5 hr. n = 3 for room temperature and n = 6 for cold.

(C) Core body temperature after a cold tolerance test at 4°C in HNF4α$^{F/F}$ mice infected with EGFP or Cre. n = 6/group.

(D) FFA levels in serum of HNF4α$^{F/F}$ mice infected with EGFP or Cre. Mice were challenged with cold or room temperature for 5 hr. n = 3 for room temperature and n = 6 for cold.

(E) Serum long-chain acylcarnitine levels as measured by LC-MS from 5-hr cold-exposed HNF4α$^{F/F}$ mice infected with EGFP or Cre. n = 6/group.

(F) ChIP-seq analysis of hepatic HNF4α in proximity to promoters of Cpt1b, Octn2, PPARα, and CrAT.

(G) Targeted ChIP-qPCR of HNF4α in the promoters of Cpt1b, Octn2, PPARα, and CrAT in the liver of 3-month-old C57BL6J male mice. n = 3.

All transcripts were normalized to RPL13. Data are presented as means ± SEM. *p ≤ 0.05, **p ≤ 0.01, ***p ≤ 0.001. See also Figure S4.

(Figure 4C). To test whether other HNF4α targets are induced by cold exposure in the liver, we measured Apoa4 expression by western blot analysis. Apoa4 increases in response to 5 or 8 hr of cold exposure (Figure S4A). Notably, HNF4α expression is unchanged through the 5-hr time course (Figure 4C). Acylcarnitine levels in the liver increase within 1 hr with levels of 12:0-,14:0-,16:0-carnitine continuing to rise during cold exposure, while 18:0-carnitine increased within the first hour and decreased thereafter (Figure 4D).

HNF4α Regulates Acylcarnitine Metabolism in the Liver of Cold-Exposed Mice

The observed increase in hepatic gene expression of enzymes involved in acylcarnitine metabolism led us to test a direct role for HNF4α in the liver, particularly with prior evidence that the nuclear receptors HNF4α and PPARα are known regulators of Cpt1 and Cpt2 expression (Gutgesell et al., 2009; Hayhurst et al., 2001; Louet et al., 2002; Martinez-Jimenez et al., 2010; Song et al., 2010). To determine whether the cold-induced changes in hepatic gene expression were due to HNF4α, we generated mice lacking HNF4α in hepatocytes (Walesky et al., 2013). HNF4α$^{F/F}$ mice received either a control adeno-associated virus 8 (AAV8)-thyroid hormone binding globin (TBG)-eGFP or AAV8-TBG-eGFP-Cre 1 week prior to cold challenge, leading to selective deletion of HNF4α in the liver (Figures 5A, 5B, and S5B). After 5 hr of cold exposure, loss of HNF4α led to impaired induction in Cpt1b, Octn2, CrAT, Apoa4, and PGC-1α when compared with AAV8-TBG-eGFP controls (Figure 5B), while basal levels of Cpt2 and CACT were reduced in HNF4α null mice. These transcriptional changes correlated with functional changes in thermogenesis. HNF4α$^{F/F}$ AAV8-TBG-eGFP-Cre mice were unable to maintain their core body temperatures when challenged with a cold tolerance test and displayed lower levels of circulating acylcarnitines (Figures 5C and 5E). The loss of HNF4α did not lead to complete disruption of circulating lipids. HNF4α$^{F/F}$ AAV8-TBG-Cre mice exhibited a similar rise in FFAs during cold exposure as the HNF4α$^{F/F}$ AAV8-TBG-eGFP control mice (Figure 5D). To determine whether other sources of energy

were depleted, we measured blood glucose levels and found an increase in mice lacking HNF4α in hepatocytes (Figure S5A). In contrast, serum triglycerides were reduced with the loss of HNF4α (Figure S5E). Notably, the expression of thermogenic genes UCP1, Elovl3, Dio2, and brown adipocyte markers, Cidea, Prdm16, and Eva1 was not altered in the BAT of hepatocyte-selective HNF4α null mice (Figure S5C). Furthermore, gene expression of acylcarnitine transcripts Cpt1b, Octn2, CACT, and CrAT was unchanged in BAT (Figure S5C).

Although Cpt1 and Cpt2 regulation by HNF4α is well established, we also observed reduction in Octn2 and CrAT expression in the livers of hepatocyte-selective HNF4α null mice (Hayhurst et al., 2001; Martinez-Jimenez et al., 2010). To determine if these changes in Octn2 and CrAT were due to direct regulation by HNF4α, we interrogated publicly available chromatin immunoprecipitation sequencing (ChIP-seq) datasets to determine whether HNF4α occupies their promoters (Alpern et al., 2014). HNF4α binding peaks were observed in proximity to promoters of PPARα, Cpt1b, Octn2, and CrAT (Figure 5F). These peaks were validated by targeted ChIP-qPCR using livers from C57BL6J mice (Figure 5G). Together these findings suggest that hepatic HNF4α is a major regulator of the cold-adaptive response in the liver.

Palmitate Treatment in Hepatocytes Activates Expression of Acylcarnitine Pathway through HNF4α

To test whether FFAs could directly stimulate the expression of HNF4α targets, we isolated HNF4α$^{F/F}$ primary hepatocytes expressing Rosa 26 LSL-tomato, which allowed us to test efficiency of Cre recombinase by detection of red fluorescent protein (Figure 6A). Hepatocytes were infected with adeno-associated virus 48 hr prior to treatment with fatty acids. Hepatocytes were incubated with BSA alone or BSA conjugated to palmitate at a concentration of 0.25, 0.5, and 1.0 mM. Palmitate treatment increased expression of HNF4α targets Octn2, Apoa4, MTTP, and PGC1α in a dose-dependent fashion, while expression of HNF4α and cyk18 was unchanged with palmitate treatment. The palmitate response was abrogated by the loss of HNF4α, as hepatocytes infected with Cre recombinase had a blunted response to palmitate *in vitro* (Figures 6B and S6A). These findings suggest that treatment of hepatocytes with FFAs is sufficient in stimulating the cold-induced transcriptional response.

Circulating Acylcarnitines Provide a Fuel Source for BAT Thermogenesis

To determine which tissues take up LCACs *in vivo*, we administered radiolabeled ^{14}C-palmitoylcarnitine by intravenous (i.v.) administration to mice exposed to room temperature or cold. The rate of ^{14}C-palmitoylcarnitine clearance from circulation occurs rapidly in cold-exposed mice; after 1 hr 18% of palmitoylcarnitine is cleared at room temperature, while 69% is cleared in the cold (Figure 6C). In the cold, mice took up 8-fold more acylcarnitines in BAT, 8-fold in skeletal muscle, and 4-fold in the heart, while uptake in inguinal WAT was reduced by 112-fold, 21-fold in epididymal WAT, and 89-fold in liver (Figure 6D). Although these results show that LCACs are being taken up by BAT, they fail to elucidate whether acylcarnitines are metabolized. Using isotopic labeling experiments, we tested whether differentiated brown adipocytes take up acylcarnitines. Brown adipocytes were incubated with 100 μM ^{12}C-palmitoylcarnitine or heavy-labeled ^{13}C-1,2,3,4-palmitoylcarnitine, and we measured the incorporation of heavy-labeled carbons into the tricarboxylic cycle (TCA) pool. We found that cells take up palmitoylcarnitine (Figure 6E), as supported by the abundance of the m + 4 isotopomer of palmitoylcarnitine. To test whether ^{13}C-1,2,3,4-palmitoylcarnitine was metabolized, we measured the incorporation of ^{13}C into the TCA intermediate citrate and found that the m + 2 isotopomer could be detected (Figure 6F). Together these findings support that palmitoylcarnitine is actively taken up by brown adipocytes and metabolized.

Reversal of Cold-Sensitive Phenotype in Aged Mice Is Rescued by Acylcarnitine Administration

As mice age, there is an impairment in thermogenic capacity (Figure S1E) and, as shown in Figure 1D, reduced acylcarnitine levels. These changes coincide with reduced hepatic expression of genes involved in acylcarnitine metabolism (Figure 7A). To test whether the reduction with aging impairs thermogenesis, we administered a single dose of 100 mg/kg of carnitine, which led to an increase in acylcarnitine levels during cold exposure (Figure 7B). We found that carnitine administration prevents hypothermia associated with aging, reversing cold sensitivity in 1-year-old mice placed at 4°C (Figure 7C) and 2.5-year-old mice placed at 16°C (Figure 7D). Carnitine administration in 2.5-year-old mice reduced core body temperature by an average of 1.5°C compared with the control group that lost 5°C (Figure 7D). Moreover, intravenous administration of palmitoylcarnitine through the tail vein was able to improve thermoregulation when mice were challenged with 16°C (Figure 7E). The bolus of carnitine did not alter BAT gene expression in the 2.5-year-old mice when we assessed UCP1, Dio2, Elovl3, and Eva1 (Figure S7B). However, the ability of carnitine to improve thermogenesis was reliant on the presence of BAT, as UCP-DTA mice that lack BAT did not respond to carnitine administration (Figure 7F). Together these findings indicate that the drop in acylcarnitines contributes to the cold-sensitive phenotype observed with aging.

DISCUSSION

Non-targeted LC-MS analysis of plasma lipids during cold exposure led to the identification of acylcarnitines as a cold-induced metabolite. While several acylcarnitine species had previously been detected in the blood in cases of inborn errors of metabolism, exercise, diabetes, and fasting, little was known about their physiologic function. Here, we show that acylcarnitine levels increase in response to the cold, are synthesized by the liver, and provide a fuel source for BAT thermogenesis. Acylcarnitine production is stimulated through the activation of the nuclear receptor HNF4α, by directly regulating the expression of genes involved in acylcarnitine metabolism. HNF4α activation requires FFA release from adipose tissue lipolysis, which provides a stimulus for HNF4α activation and substrate for acylcarnitine synthesis. Blocking acylcarnitine production in the liver reduces serum acylcarnitine levels and impairs their ability to adapt to the cold. It has been well documented in rodents and humans that aging impairs thermogenesis; however, little is known about the mechanisms at play. Here, we found that

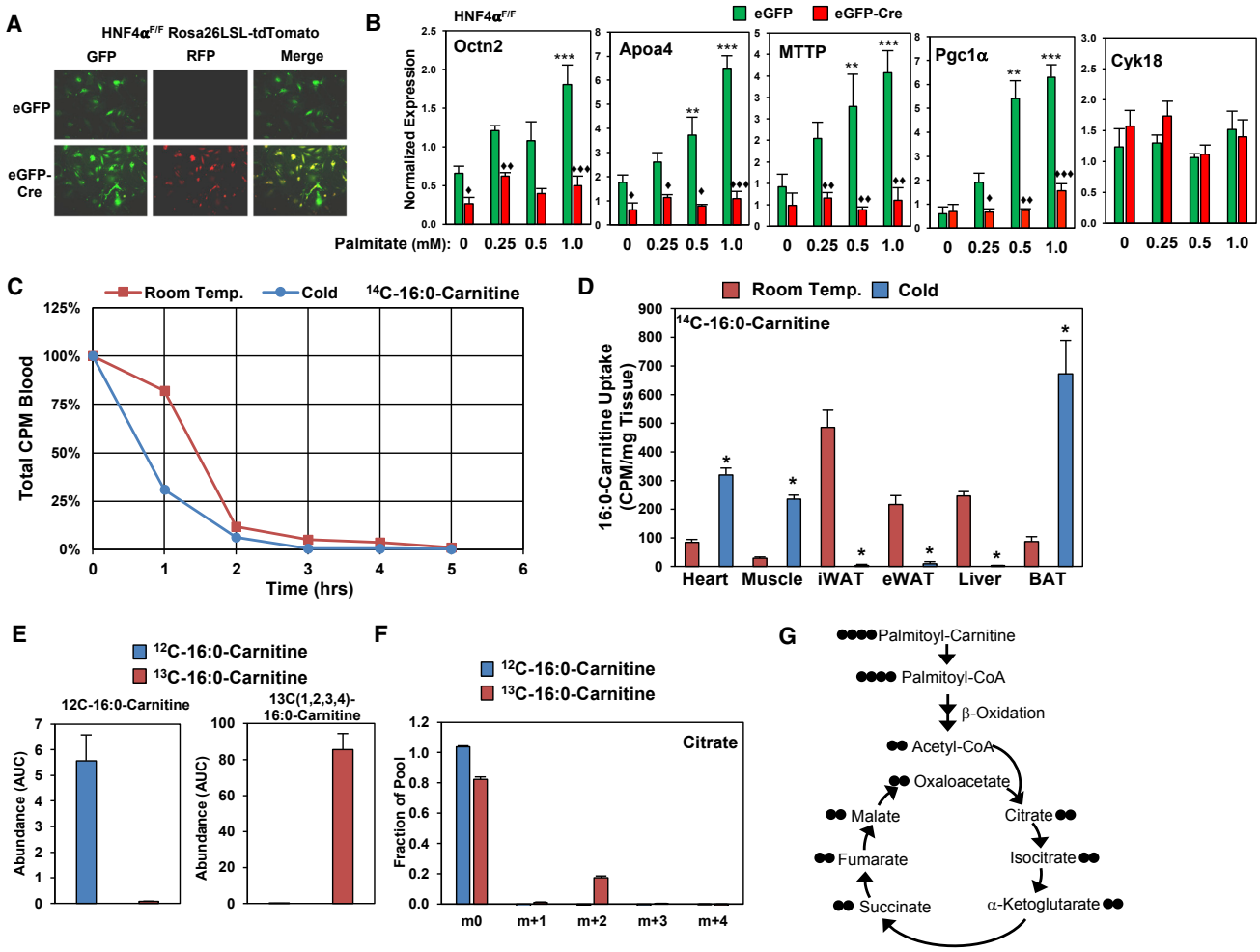

Figure 6. Acylcarnitines Are Taken Up by BAT and Metabolized through the TCA Cycle

(A) Hepatocytes from HNF4α$^{F/F}$ mice expressing Rosa26-LSL-tdTomato infected with adenoviral CMV-eGFP (EGFP) or CMV-eGFP-Cre (Cre). Cre-induced recombination leads to expression of red fluorescent protein (RFP). Hepatocytes were infected for 16 hr 2 days prior to harvest.

(B) Gene expression changes in hepatocytes measured by real-time PCR after treatment with BSA or BSA/palmitate at 0.25, 0.5, and 1.0 mM for 6 hr. n = 3/group.

(C) Clearance of U-^{14}C-palmitoylcarnitine from the blood of C57BL6J male mice placed at room temperature (24°C) or cold (4°C). N = 4/group. Mice received a single intravenous dose of U-^{14}C-palmitoylcarnitine.

(D) Tissue uptake of U-^{14}C-palmitoylcarnitine 5 hr post injection in mice placed at room temperature or cold. n = 4/group.

(E) Uptake of heavy-labeled palmitoylcarnitine as measured by gas chromatography-MS in differentiated brown adipocytes incubated with either ^{12}C-16:0-carnitine or ^{13}C-(1,2,3,4)-16:0-carnitine for 6 hr. n = 5/group.

(F) Incorporation of ^{13}C-(1,2,3,4)-16:0-carnitine into the TCA cycle intermediate m + 2 citrate. n = 5/group.

(G) Schematic of ^{13}C-(1,2,3,4)-16:0-carnitine entry and incorporation into the TCA cycle.

All transcripts were normalized to RPL13. Data are presented as means ± SEM. For comparison of HNF4α$^{F/F}$ EGFP between BSA control (0) and palmitate treatment, *p ≤ 0.05, **p ≤ 0.01, ***p ≤ 0.001. n = 5. For comparison between EGFP and Cre-infected cells of the same treatment groups, ◆p ≤ 0.05, ◆◆p ≤ 0.01, ◆◆◆p ≤ 0.001 See also Figure S6.

induction of acylcarnitine levels in response to cold exposure were blunted in older mice. The cold-sensitive phenotype observed can be reversed with carnitine administration, a treatment that is known to stimulate acylcarnitine production. Furthermore, infusing palmitoylcarnitine alone can improve core body temperature when aged mice are challenged with cold exposure. In sum, these findings indicate that the liver is an integral component of adaptive thermogenesis, as well as uncovering a well-orchestrated inter-tissue communication system to upregulate energy mobilization for heat production.

The liver is a focal point for energy mobilization, providing ketones and glucose during fasting, as well as packaging lipid-rich lipoproteins for peripheral tissues. Acylcarnitines in the plasma have traditionally been thought of as markers of metabolic stress (Burrage et al., 2016; Genuth and Hoppel, 1981; Mai et al., 2013; McCoin et al., 2015; Schooneman et al., 2013). Although serum acylcarnitines fluctuate, a functional role for circulating acylcarnitines has yet to be determined. Using radiolabeled palmitoylcarnitine, we found increased uptake in the BAT, skeletal muscle, and heart during cold exposure,

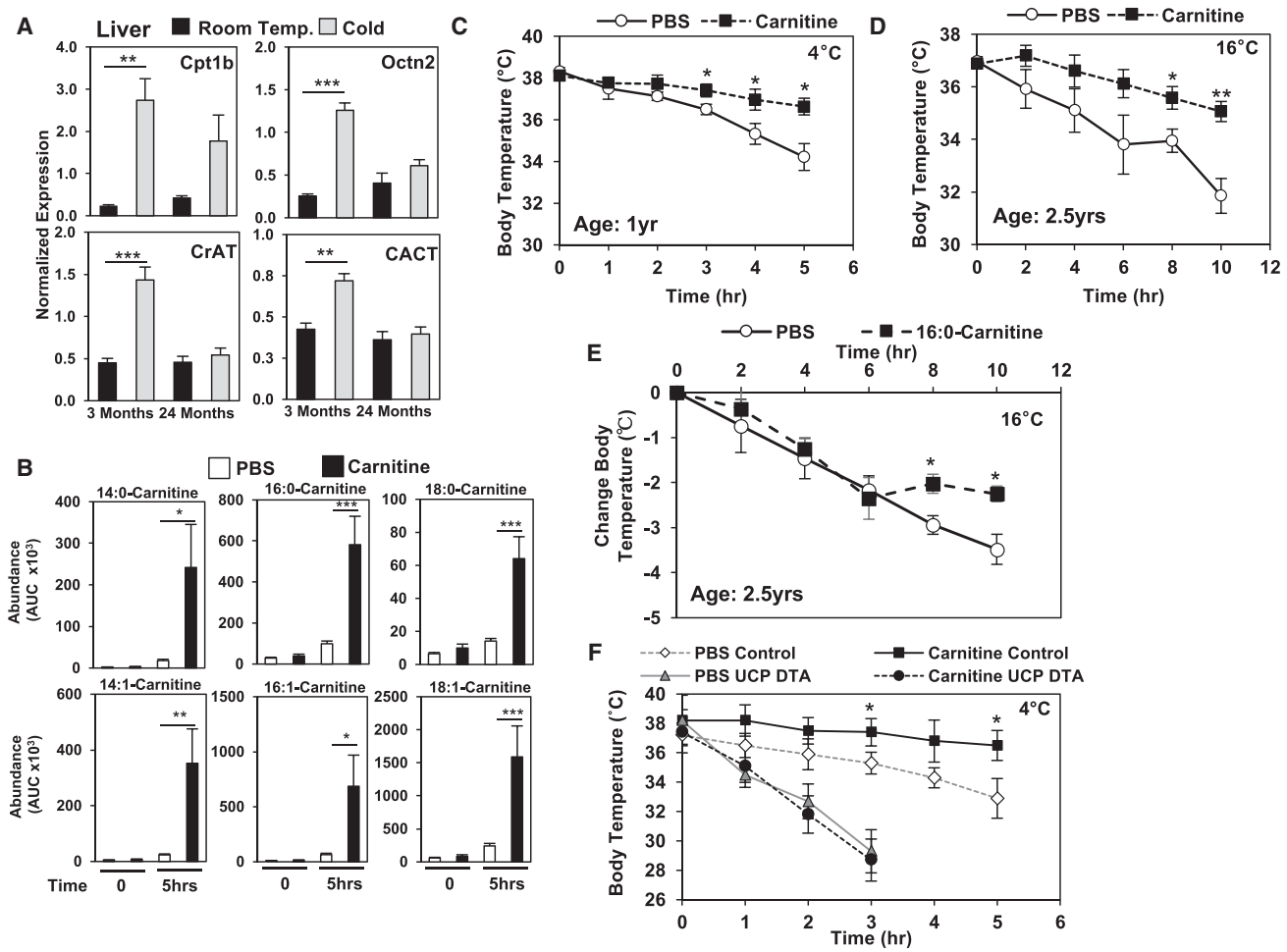

Figure 7. Carnitine Treatment Stimulates Acylcarnitine Production and Protects against Age-Induced Cold Sensitivity

(A) Hepatic gene expression in 3-month-old and 24-month-old mice exposed to room temperature (24°C) or cold (4°C). n = 5/group

(B) Treatment of 2.5-year-old mice with carnitine (100 mg/kg body weight) increases their serum acylcarnitine levels after 5 hr of cold as measured by LC-MS. n = 5/group.

(C) Core body temperature after cold tolerance test at 4°C in 12-month-old mice treated with either PBS or 100 mg/kg carnitine. n = 5/group.

(D) Core body temperature after cold tolerance test at 16°C in 2.5-year-old mice treated with either PBS or 100 mg/kg carnitine. n = 5/group.

(E) Change in core body temperature in 2.5-year-old mice treated with PBS or 16:0-carnitine (100 μM). n = 5/group.

(F) Core body temperature of littermate control and UCP-DTA transgenic mice treated with PBS or with 100 mg/kg carnitine. n = 5/group.

Data are presented as means ± SEM. *p ≤ 0.05, **p ≤ 0.01, ***p ≤ 0.001. n = 5. See also Figure S7.

indicating that acylcarnitines are utilized by multiple tissues through a tightly controlled mechanism. Notably, uptake of acylcarnitines decreased in WAT and liver in response to the cold, presumably to direct acylcarnitines toward metabolically active tissues. The active regulation of palmitoylcarnitine uptake suggests a role for acylcarnitines beyond markers of metabolic stress. Uptake was also detected in brown adipocytes *in vitro* using the metabolic tracer ^{13}C-1,2,3,4-palmitoylcarnitine. These studies showed that acylcarnitines were taken up by brown adipocytes and metabolized, an outcome that was supported by the heavy labeling of the TCA intermediate citrate. Alternatively, acylcarnitines may improve thermoregulation through metabolic flux in the liver, producing heat as a byproduct of acylcarnitine synthesis. Early studies suggest that hepatic thermogenesis is possible, an outcome that was previously measured by calorimetry and shown to contribute to the total body temperature (Baconnier et al., 1979). Further studies are needed to determine the input of hepatic lipid processing in thermoregulation during cold exposure. However, our result that palmitoylcarnitine alone is sufficient to enhance thermogenesis indicates that acylcarnitines are capable of modulating thermogenesis independently of their synthesis, and the failure of carnitine to rescue cold sensitivity in the UCP-DTA mice suggests that liver processing is not sufficient to improve hypothermia. Together these results support a model that acylcarnitines are a fuel source for thermogenesis, but it is important to note that these studies do not rule out the possibility of acylcarnitines having a signaling role as well.

There is a prevailing view that FFAs are the major source of energy for thermogenesis, yet we find that acylcarnitine

production is required as shown by knockdown studies of hepatic Cpt1a/b that leads to reduced blood acylcarnitine levels, suggesting that this long-held view is overly simplistic. This is also supported by the observation that deletion of hepatic HNF4α leads to reduced acylcarnitine levels, while FFA levels are unchanged, suggesting that FFAs are not sufficient for thermogenesis. This finding is surprising, considering the high abundance of FFAs that are available for thermogenesis in response to the cold. However, the metabolic program of brown adipocytes is unique compared with other cell types, where its activation leads to enhanced fatty acid oxidation, glucose uptake and utilization, lipogenesis, and lipolysis. This unique metabolic program reflects the dualistic nature of BAT that is capable of storing excess lipids similarly to other adipose depots and yet shares similar features with skeletal muscle, including high mitochondrial content and high capacity for fatty acid oxidation (Festuccia et al., 2011; Yu et al., 2002). In other tissues, fuel selection is regulated by the Randle cycle, a series of inhibitory signals that regulate glucose or fatty acid utilization, a process driven by substrate availability (Hue and Taegtmeyer, 2009). In the Randle cycle, when both glucose and fatty acids are readily available, the TCA cycle intermediate citrate is exported to the cytoplasm to ultimately generate malonyl-CoA, an inhibitor of Cpt1b, the rate-limiting step in fatty acid oxidation. Through inhibition of fatty acid oxidation, this allows the preferential use of glucose for energy (McGarry et al., 1991). Although cold exposure is energetically demanding, there is a high abundance of peripheral fuel sources, including serum glucose, FFAs, and triglycerides (Bartelt et al., 2011; Kinoshita et al., 2014; Wu et al., 2006). During acute cold exposure, malonyl-CoA levels in BAT rise to levels that would inhibit Cpt1b activity (Saggerson and Carpenter, 1982). These conditions suggest that initial BAT thermogenesis is dependent on glucose uptake and perhaps other fuel sources such as triglycerides, while persistent cold challenge may require a switch toward utilizing energetically rich molecules such as acylcarnitines. Therefore, we propose a model in which acylcarnitines provide a mechanism for lipid utilization to bypass the inhibition of Cpt1b in brown adipocytes, expediting the metabolic switch to FFA utilization.

The increase in expression of genes involved in acylcarnitine metabolism in response to cold was surprising, as there is little evidence for the liver's involvement in adaptive thermogenesis. Prior studies on the transcriptional regulation of Cpt1 led our focus to HNF4α, which is primarily thought to be involved in liver development. Analysis of HNF4α occupancy using publicly available ChIP-seq datasets revealed potential binding sites in the promoter region of other genes involved in acylcarnitine metabolism (Louet et al., 2002; Martinez-Jimenez et al., 2010). Notably, HNF4α binding at these sites did not change in response to the cold, an outcome noted by other HNF4α targets (data not shown); instead, it is the binding to various coactivators that likely drives changes in HNF4α activity. HNF4α activity is largely driven by coregulator interactions, where Hes6 has been shown to be inhibitory, while interactions through PGC-1α activate transcription (Martinez-Jimenez et al., 2010; Rhee et al., 2003, 2006). We found that in response to the cold, expression of hepatic PGC-1α was induced but lost as mice aged. The induction of PGC1α is likely driven by FFAs, which stimulate CREB phosphorylation and increase expression of PGC1α. These findings fit with our model that HNF4α activation is dependent on the FFA release observed with the cold or activation with a β3-AR agonist CL-316,243 (Collins et al., 2006; Herzig et al., 2001; Schauer and Reusch, 2009). Alternatively, FFAs could activate HNF4α directly through its ligand-binding domain, although binding of HNF4α to its purported lipid ligand has been shown to occur during assembly, while others have shown linoleic acid regulates HNF4α activity (Dhe-Paganon et al., 2002; Yuan et al., 2009). Our studies indicate that HNF4α is required for the induction of PGC1α, Octn2, MTTP, and Apoa4 in response to palmitate in hepatocytes. Additional studies are needed to understand the mechanism through which cold exposure increases HNF4α activity as well as other regulatory elements controlling this cold response in the liver. Although the induction of genes involved in acylcarnitine metabolism is abrogated in HNF4α knockout livers, they are not completely ablated. This suggests that other transcriptional regulators are involved in mediating the cold response observed with Octn2, Cpt2, CACT, and CrAT. Together our findings support a model in which FFA release during the cold stimulates a transcriptional program driven by HNF4α, ultimately leading to acylcarnitine synthesis and release into the plasma. This model explains why the β3-AR agonist CL-316,243 stimulates acylcarnitine levels in the blood, despite the lack of β3-AR expression in hepatocytes.

The source of serum acylcarnitines has long been a mystery. We found that a rise in acylcarnitines is dependent on the increase in circulating FFAs from adipose tissue. Inhibition of adipose tissue triglyceride lipolysis, by selective deletion of ATGL in adipocytes, blocked the increase in circulating acylcarnitines in response to β3-AR agonist. Acute inhibition of ATGL with Atglistatin treatment also led to cold intolerance in mice and reduced levels of acylcarnitines and induction of hepatic gene expression. Although Atglistatin treatment inhibits ATGL in multiple tissues, others have shown that ATGL knockout mice are sensitive to hypothermia and that loss of ATGL in the adipocytes is sufficient to decrease β3-AR agonist stimulation of FFA release (Ahmadian et al., 2011; Haemmerle et al., 2006). Interestingly, both adipose-selective deletion of ATGL and Atglistatin treatment inhibited the increased expression of hepatic acylcarnitine transcripts, suggesting that the cold-induced FFAs are not only acting as a substrate for acylcarnitine synthesis but also stimulate the cold-induced transcriptional program in the liver. This observation is recapitulated *in vitro* with palmitate treatment of hepatocytes.

Our studies aimed to develop a deeper understanding of the metabolic changes that take place with cold exposure. Together, our findings support a model that acylcarnitines are synthesized by the liver to provide fuel for peripheral tissues during cold exposure. The inability to generate acylcarnitines by the liver leads to hypothermia. The rise in acylcarnitines is driven by substrate availability of FFAs through adipose tissue lipolysis and FFA activation of hepatic HNF4α, which drives the expression of genes involved in acylcarnitine production. In response to the cold, there is partitioning of acylcarnitines to BAT, heart, and skeletal muscle, while liver and WAT decrease uptake. Notably, brown adipocytes take up and catabolize acylcarnitines. This broadens the understanding of the liver as a metabolic hub that processes fuel for peripheral tissues, including hepatic gluconeogenesis, lipoprotein synthesis, ketogenesis, and now

acylcarnitine production. In sum, these studies demonstrate the importance of peripheral energy sources in heat production by brown adipocytes and discovered an inter-tissue communication system that regulates thermogenesis.

STAR★METHODS

Detailed methods are provided in the online version of this paper and include the following:

- KEY RESOURCES TABLE
- CONTACT FOR REAGENT AND RESOURCE SHARING
- EXPERIMENTAL MODEL AND SUBJECT DETAILS
  - Animal Care
  - Genetic Mouse Models
  - Brown Adipocyte
  - Primary Hepatocytes
- METHOD DETAILS
  - Cold Exposure
  - CL-316,243 Administration
  - Atglistatin Treatment
  - Carnitine and Palmitoylcarnitine Administration
  - Palmitate Treatment of Primary Hepatocytes
  - Tissue Uptake of Palmitoylcarnitine
  - Brown Adipocyte ^{13}C-1,2,3,4-palmitoylcarnitine Labeling
  - Hepatic Knockdown Studies
  - Lipid Measurements
  - Acylcarnitine Analysis
  - Metabolic Tracer Analysis
  - Gene Expression
  - Protein Analysis
  - Chromatin Immunoprecipitation
- QUANTIFICATION AND STATISTICAL ANALYSIS

SUPPLEMENTAL INFORMATION

Supplemental Information includes seven figures and three tables and can be found with this article online at http://dx.doi.org/10.1016/j.cmet.2017.08.006.

AUTHOR CONTRIBUTIONS

J.S., C.J.V., G.G., J.A.M., C.L.B., M.P., R.M., S.L., I.H., R.S., and J.C. conducted experiments; J.S., A.J.D., U.A., L.J., N.L., E.E.K., J.R., R.Z., and C.J.V. designed experiments; and J.S. and C.J.V. wrote paper. All authors contributed to data analysis.

ACKNOWLEDGMENTS

The authors are grateful to members of the Diabetes and Metabolism Center and the Biochemistry Department at the University of Utah for useful discussion and feedback. Lipidomics and metabolic tracer analysis was performed at the Metabolomics Core Facility at the University of Utah. This study was supported by NIDDK KO1DK097285, NIDDK RO3DK103089, NIDDK RO1DK103930, Margolis Research Foundation, NIDDK DRC, T32DK091317, and S10 OD016232-01. The content is solely the responsibility of the authors and does not necessarily represent the official views of the NIH.

Received: August 29, 2016
Revised: April 27, 2017
Accepted: August 8, 2017
Published: September 5, 2017

REFERENCES

Ahmadian, M., Abbott, M.J., Tang, T., Hudak, C.S.S., Kim, Y., Bruss, M., Hellerstein, M.K., Lee, H.-Y., Samuel, V.T., Shulman, G.I., et al. (2011). Desnutrin/ATGL is regulated by AMPK and is required for a brown adipose phenotype. Cell Metab. *13*, 739–748.

Alpern, D., Langer, D., Ballester, B., Le Gras, S., Romier, C., Mengus, G., and Davidson, I. (2014). TAF4, a subunit of transcription factor II D, directs promoter occupancy of nuclear receptor HNF4A during post-natal hepatocyte differentiation. Elife *3*, e03613.

Baconnier, P., Benchetrit, G., and Tanche, M. (1979). Liver heat production and temperature regulation in the anesthetized dog. Am. J. Physiol. *237*, R334–R339.

Bartelt, A., Bruns, O.T., Reimer, R., Hohenberg, H., Ittrich, H., Peldschus, K., Kaul, M.G., Tromsdorf, U.I., Weller, H., Waurisch, C., et al. (2011). Brown adipose tissue activity controls triglyceride clearance. Nat. Med. *17*, 200–205.

Bukong, T.N., Momen-Heravi, F., Kodys, K., Bala, S., and Szabo, G. (2014). Exosomes from hepatitis C infected patients transmit HCV infection and contain replication competent viral RNA in complex with Ago2-miR122-HSP90. PLoS Pathog. *10*, e1004424.

Burrage, L.C., Miller, M.J., Wong, L.J., Kennedy, A.D., Sutton, V.R., Sun, Q., Elsea, S.H., and Graham, B.H. (2016). Elevations of C14:1 and C14:2 plasma acylcarnitines in fasted children: a diagnostic dilemma. J. Pediatr. *169*, 208–213.e2.

Cannon, B., Hedin, A., and Nedergaard, J. (1982). Exclusive occurrence of thermogenin antigen in brown adipose tissue. FEBS Lett. *150*, 129–132.

Chondronikola, M., Volpi, E., Børsheim, E., Porter, C., Annamalai, P., Enerbäck, S., Lidell, M.E., Saraf, M.K., Labbe, S.M., Hurren, N.M., et al. (2014). Brown adipose tissue improves whole-body glucose homeostasis and insulin sensitivity in humans. Diabetes *63*, 4089–4099.

Collins, Q.F., Xiong, Y., Lupo, E.G., Jr., Liu, H.Y., and Cao, W. (2006). p38 Mitogen-activated protein kinase mediates free fatty acid-induced gluconeogenesis in hepatocytes. J. Biol. Chem. *281*, 24336–24344.

Costa, C.C., de Almeida, I.T., Jakobs, C., Poll-The, B.T., and Duran, M. (1999). Dynamic changes of plasma acylcarnitine levels induced by fasting and sunflower oil challenge test in children. Pediatr. Res. *46*, 440–444.

Dhe-Paganon, S., Duda, K., Iwamoto, M., Chi, Y.I., and Shoelson, S.E. (2002). Crystal structure of the HNF4 alpha ligand binding domain in complex with endogenous fatty acid ligand. J. Biol. Chem. *277*, 37973–37976.

Esser, V., Britton, C.H., Weis, B.C., Foster, D.W., and McGarry, J.D. (1993). Cloning, sequencing, and expression of a cDNA encoding rat liver carnitine palmitoyltransferase I. Direct evidence that a single polypeptide is involved in inhibitor interaction and catalytic function. J. Biol. Chem. *268*, 5817–5822.

Festuccia, W.T., Blanchard, P.-G., and Deshaies, Y. (2011). Control of brown adipose tissue glucose and lipid metabolism by PPARγ. Front. Endocrinol. *2*, 84.

Fingerhut, R., Roschinger, W., Muntau, A.C., Dame, T., Kreischer, J., Arnecke, R., Superti-Furga, A., Troxler, H., Liebl, B., Olgemoller, B., et al. (2001). Hepatic carnitine palmitoyltransferase I deficiency: acylcarnitine profiles in blood spots are highly specific. Clin. Chem. *47*, 1763–1768.

Gempel, K., Kiechl, S., Hofmann, S., Lochmuller, H., Kiechl-Kohlendorfer, U., Willeit, J., Sperl, W., Rettinger, A., Bieger, I., Pongratz, D., et al. (2002). Screening for carnitine palmitoyltransferase II deficiency by tandem mass spectrometry. J. Inherit. Metab. Dis. *25*, 17–27.

Genuth, S.M., and Hoppel, C.L. (1981). Acute hormonal effects on carnitine metabolism in thin and obese subjects: responses to somatostatin, glucagon, and insulin. Metabolism *30*, 393–401.

Golozoubova, V., Hohtola, E., Matthias, A., Jacobsson, A., Cannon, B., and Nedergaard, J. (2001). Only UCP1 can mediate adaptive nonshivering thermogenesis in the cold. FASEB J. *15*, 2048–2050.

Gutgesell, A., Ringseis, R., Schmidt, E., Brandsch, C., Stangl, G.I., and Eder, K. (2009). Downregulation of peroxisome proliferator-activated receptor alpha and its coactivators in liver and skeletal muscle mediates the metabolic adaptations during lactation in mice. J. Mol. Endocrinol. *43*, 241–250.

Haemmerle, G., Lass, A., Zimmermann, R., Gorkiewicz, G., Meyer, C., Rozman, J., Heldmaier, G., Maier, R., Theussl, C., Eder, S., et al. (2006). Defective lipolysis and altered energy metabolism in mice lacking adipose triglyceride lipase. Science *312*, 734–737.

Haemmerle, G., Moustafa, T., Woelkart, G., Büttner, S., Schmidt, A., van de Weijer, T., Hesselink, M., Jaeger, D., Kienesberger, P.C., Zierler, K., et al. (2011). ATGL-mediated fat catabolism regulates cardiac mitochondrial function via PPAR-α and PGC-1. Nat. Med. *17*, 1076–1085.

Hayashi, Y., Mori, Y., Janssen, O.E., Sunthornthepvarakul, T., Weiss, R.E., Takeda, K., Weinberg, M., Seo, H., Bell, G.I., and Refetoff, S. (1993). Human thyroxine-binding globulin gene: complete sequence and transcriptional regulation. Mol. Endocrinol. *7*, 1049–1060.

Hayhurst, G.P., Lee, Y.H., Lambert, G., Ward, J.M., and Gonzalez, F.J. (2001). Hepatocyte nuclear factor 4alpha (nuclear receptor 2A1) is essential for maintenance of hepatic gene expression and lipid homeostasis. Mol. Cell. Biol. *21*, 1393–1403.

Herzig, S., Long, F., Jhala, U.S., Hedrick, S., Quinn, R., Bauer, A., Rudolph, D., Schutz, G., Yoon, C., Puigserver, P., et al. (2001). CREB regulates hepatic gluconeogenesis through the coactivator PGC-1. Nature *413*, 179–183.

Hiatt, W.R., Regensteiner, J.G., Wolfel, E.E., Ruff, L., and Brass, E.P. (1989). Carnitine and acylcarnitine metabolism during exercise in humans. Dependence on skeletal muscle metabolic state. J. Clin. Invest. *84*, 1167–1173.

Himms-Hagen, J., Cui, J., Danforth, E., Jr., Taatjes, D.J., Lang, S.S., Waters, B.L., and Claus, T.H. (1994). Effect of CL-316,243, a thermogenic beta 3-agonist, on energy balance and brown and white adipose tissues in rats. Am. J. Physiol. *266*, R1371–R1382.

Hue, L., and Taegtmeyer, H. (2009). The Randle cycle revisited: a new head for an old hat. Am. J. Physiol. Endocrinol. Metab. *297*, E578–E591.

Katajamaa, M., and Orešič, M. (2005). Processing methods for differential analysis of LC/MS profile data. BMC Bioinformatics *6*, 179.

Kinoshita, K., Ozaki, N., Takagi, Y., Murata, Y., Oshida, Y., and Hayashi, Y. (2014). Glucagon is essential for adaptive thermogenesis in brown adipose tissue. Endocrinology *155*, 3484–3492.

Lafontan, M., and Berlan, M. (1993). Fat cell adrenergic receptors and the control of white and brown fat cell function. J. Lipid Res. *34*, 1057–1091.

Liu, A., and Pasquali, M. (2005). Acidified acetonitrile and methanol extractions for quantitative analysis of acylcarnitines in plasma by stable isotope dilution tandem mass spectrometry. J. Chromatogr. B Analyt Technol. Biomed. Life Sci. *827*, 193–198.

Longo, N., di San Filippo, C.A., and Pasquali, M. (2006). Disorders of carnitine transport and the carnitine cycle. Am. J. Med. Genet. C Semin. Med. Genet. *142C*, 77–85.

Louet, J.F., Hayhurst, G., Gonzalez, F.J., Girard, J., and Decaux, J.F. (2002). The coactivator PGC-1 is involved in the regulation of the liver carnitine palmitoyltransferase I gene expression by cAMP in combination with HNF4 alpha and cAMP-response element-binding protein (CREB). J. Biol. Chem. *277*, 37991–38000.

Lowell, B.B., S-Susulic, V., Hamann, A., Lawitts, J.A., Himms-Hagen, J., Boyer, B.B., Kozak, L.P., and Flier, J.S. (1993). Development of obesity in transgenic mice after genetic ablation of brown adipose tissue. Nature *366*, 740–742.

Mai, M., Tonjes, A., Kovacs, P., Stumvoll, M., Fiedler, G.M., and Leichtle, A.B. (2013). Serum levels of acylcarnitines are altered in prediabetic conditions. PLoS One *8*, e82459.

Martinez-Jimenez, C.P., Kyrmizi, I., Cardot, P., Gonzalez, F.J., and Talianidis, I. (2010). Hepatocyte nuclear factor 4α coordinates a transcription factor network regulating hepatic fatty acid metabolism. Mol. Cell. Biol. *30*, 565–577.

Mayer, N., Schweiger, M., Romauch, M., Grabner, G.F., Eichmann, T.O., Fuchs, E., Ivkovic, J., Heier, C., Mrak, I., Lass, A., et al. (2013). Development of small-molecule inhibitors targeting adipose triglyceride lipase. Nat. Chem. Biol. *9*, 785–787.

McCoin, C.S., Knotts, T.A., and Adams, S.H. (2015). Acylcarnitines–old actors auditioning for new roles in metabolic physiology. Nat. Rev. Endocrinol. *11*, 617–625.

McGarry, J.D., Sen, A., Esser, V., Woeltje, K.F., Weis, B., and Foster, D.W. (1991). New insights into the mitochondrial carnitine palmitoyltransferase enzyme system. Biochimie *73*, 77–84.

Mu, X., Español-Suñer, R., Mederacke, I., Affò, S., Manco, R., Sempoux, C., Lemaigre, F.P., Adili, A., Yuan, D., Weber, A., et al. (2015). Hepatocellular carcinoma originates from hepatocytes and not from the progenitor/biliary compartment. J. Clin. Invest. *125*, 3891–3903.

Orava, J., Nuutila, P., Lidell, M.E., Oikonen, V., Noponen, T., Viljanen, T., Scheinin, M., Taittonen, M., Niemi, T., Enerback, S., et al. (2011). Different metabolic responses of human brown adipose tissue to activation by cold and insulin. Cell Metab. *14*, 272–279.

Pandey, M.K., Belanger, A.P., Wang, S., and DeGrado, T.R. (2012). Structure dependence of long-chain [(18)F]fluorothia fatty acids as myocardial fatty acid oxidation probes. J. Med. Chem. *55*, 10674–10684.

Ramsay, R.R., Gandour, R.D., and van der Leij, F.R. (2001). Molecular enzymology of carnitine transfer and transport. Biochim. Biophys. Acta *1546*, 21–43.

Rhee, J., Ge, H., Yang, W., Fan, M., Handschin, C., Cooper, M., Lin, J., Li, C., and Spiegelman, B.M. (2006). Partnership of PGC-1alpha and HNF4alpha in the regulation of lipoprotein metabolism. J. Biol. Chem. *281*, 14683–14690.

Rhee, J., Inoue, Y., Yoon, J.C., Puigserver, P., Fan, M., Gonzalez, F.J., and Spiegelman, B.M. (2003). Regulation of hepatic fasting response by PPARgamma coactivator-1alpha (PGC-1): requirement for hepatocyte nuclear factor 4alpha in gluconeogenesis. Proc. Natl. Acad. Sci. USA *100*, 4012–4017.

Riches, A.C., Sharp, J.G., Thomas, D.B., and Smith, S.V. (1973). Blood volume determination in the mouse. J. Physiol. *228*, 279–284.

Rodriguez-Cuenca, S., Monjo, M., Frontera, M., Gianotti, M., Proenza, A.M., and Roca, P. (2007). Sex steroid receptor expression profile in brown adipose tissue. Effects of hormonal status. Cell Physiol. Biochem. *20*, 877–886.

Saggerson, E.D., and Carpenter, C.A. (1982). Sensitivity of brown-adipose-tissue carnitine palmitoyltransferase to inhibition by malonyl-CoA. Biochem. J. *204*, 373–375.

Schauer, I.E., and Reusch, J.E.B. (2009). Non-esterified fatty acid exposure activates protective and mitogenic pathways in vascular smooth muscle cells by alternate signaling pathways. Metabolism *58*, 319–327.

Schoiswohl, G., Stefanovic-Racic, M., Menke, M.N., Wills, R.C., Surlow, B.A., Basantani, M.K., Sitnick, M.T., Cai, L., Yazbeck, C.F., Stolz, D.B., et al. (2015). Impact of reduced ATGL-mediated adipocyte lipolysis on obesity-associated insulin resistance and inflammation in male mice. Endocrinology *156*, 3610–3624.

Schooneman, M.G., Vaz, F.M., Houten, S.M., and Soeters, M.R. (2013). Acylcarnitines: reflecting or inflicting insulin resistance? Diabetes *62*, 1–8.

Seale, P., Kajimura, S., and Spiegelman, B.M. (2009). Transcriptional control of brown adipocyte development and physiological function–of mice and men. Genes Dev. *23*, 788–797.

Sellayah, D., and Sikder, D. (2014). Orexin restores aging-related brown adipose tissue dysfunction in male mice. Endocrinology *155*, 485–501.

Severgnini, M., Sherman, J., Sehgal, A., Jayaprakash, N.K., Aubin, J., Wang, G., Zhang, L., Peng, C.G., Yucius, K., Butler, J., et al. (2012). A rapid two-step method for isolation of functional primary mouse hepatocytes: cell characterization and asialoglycoprotein receptor based assay development. Cytotechnology *64*, 187–195.

Shekhawat, P.S., Matern, D., and Strauss, A.W. (2005). Fetal fatty acid oxidation disorders, their effect on maternal health and neonatal outcome: impact of expanded newborn screening on their diagnosis and management. Pediatr. Res. *57*, 78R–86R.

Song, S., Attia, R.R., Connaughton, S., Niesen, M.I., Ness, G.C., Elam, M.B., Hori, R.T., Cook, G.A., and Park, E.A. (2010). Peroxisome proliferator activated receptor alpha (PPARalpha) and PPAR gamma coactivator (PGC-1alpha)

induce carnitine palmitoyltransferase IA (CPT-1A) via independent gene elements. Mol. Cell Endocrinol. *325*, 54–63.

Tamai, I., Ohashi, R., Nezu, J., Yabuuchi, H., Oku, A., Shimane, M., Sai, Y., and Tsuji, A. (1998). Molecular and functional identification of sodium ion-dependent, high affinity human carnitine transporter OCTN2. J. Biol. Chem. *273*, 20378–20382.

Tusher, V.G., Tibshirani, R., and Chu, G. (2001). Significance analysis of microarrays applied to the ionizing radiation response. Proc. Natl. Acad. Sci. USA *98*, 5116–5121.

Vila-Brau, A., De Sousa-Coelho, A.L., Goncalves, J.F., Haro, D., and Marrero, P.F. (2013). Fsp27/CIDEC is a CREB target gene induced during early fasting in liver and regulated by FA oxidation rate. J. Lipid Res. *54*, 592–601.

Walesky, C., Edwards, G., Borude, P., Gunewardena, S., O'Neil, M., Yoo, B., and Apte, U. (2013). Hepatocyte nuclear factor 4 alpha deletion promotes diethylnitrosamine-induced hepatocellular carcinoma in mice. Hepatology *57*, 2480–2490.

Wu, Q., Kazantzis, M., Doege, H., Ortegon, A.M., Tsang, B., Falcon, A., and Stahl, A. (2006). Fatty acid transport protein 1 is required for nonshivering thermogenesis in brown adipose tissue. Diabetes *55*, 3229–3237.

Xia, J., Sinelnikov, I.V., Han, B., and Wishart, D.S. (2015). MetaboAnalyst 3.0–making metabolomics more meaningful. Nucleic Acids Res. *43*, W251–W257.

Yamagata, K., Furuta, H., Oda, N., Kaisaki, P.J., Menzel, S., Cox, N.J., Fajans, S.S., Signorini, S., Stoffel, M., and Bell, G.I. (1996). Mutations in the hepatocyte nuclear factor-4alpha gene in maturity-onset diabetes of the young (MODY1). Nature *384*, 458–460.

Yamaguti, K., Kuratsune, H., Watanabe, Y., Takahashi, M., Nakamoto, I., Machii, T., Jacobsson, G., Onoe, H., Matsumura, K., Valind, S., et al. (1996). Acylcarnitine metabolism during fasting and after refeeding. Biochem. Biophys. Res. Commun. *225*, 740–746.

Yoneshiro, T., Aita, S., Matsushita, M., Okamatsu-Ogura, Y., Kameya, T., Kawai, Y., Miyagawa, M., Tsujisaki, M., and Saito, M. (2011). Age-related decrease in cold-activated brown adipose tissue and accumulation of body fat in healthy humans. Obesity (Silver Spring) *19*, 1755–1760.

Yu, X.X., Lewin, D.A., Forrest, W., and Adams, S.H. (2002). Cold elicits the simultaneous induction of fatty acid synthesis and beta-oxidation in murine brown adipose tissue: prediction from differential gene expression and confirmation in vivo. FASEB J. *16*, 155–168.

Yuan, X., Ta, T.C., Lin, M., Evans, J.R., Dong, Y., Bolotin, E., Sherman, M.A., Forman, B.M., and Sladek, F.M. (2009). Identification of an endogenous ligand bound to a native orphan nuclear receptor. PLoS One *4*, e5609.

STAR★METHODS

KEY RESOURCES TABLE

REAGENT or RESOURCE	SOURCE	IDENTIFIER
Antibodies		
Octn2 Antibody Rabbit Polyclonal	ProteinTech	Cat#16331-1-AP; RRID: AB_2191406
CPT1B-Specific Antibody	ProteinTech	Cat# 22170-1-AP
ApoA4 (1D6B6) Mouse mAb	Cell Signaling	Cat# 5700S; RRID: AB_10859038
β-Actin (8H10D10) Mouse mAb	Cell Signaling	Cat# 3700S; RRID: AB_2242334
Human HNF-4 alpha/NR2A1 Antibody	R & D Systems	Product# PP-H1415-00; RRID: AB_2263954
Anti-CPT1A antibody [8F6AE9]	Abcam	Cat# ab128568; RRID: AB_11141632
IgG, Rabbit	Millipore-Sigma	Cat# PP64; RRID: AB_97852
Bacterial and Virus Strains		
pBABE-hygro SV40 LT; modified from pBABE-puro SV40 LT	Addgene	Addgene #13970
VQAd CMVeGFP-2.6del 112912	ViraQuest	MSRN# 19222
VQAd CMV-Cre-eGFP	ViraQuest	MSRN# 7152
AAV8-TBG-CRE	University of Pennsylvania Vector Core	AV-8-PV1091
AAV8-TBG-eGFP	University of Pennsylvania Vector Core	AV-8-PV0146
Chemicals, Peptides, and Recombinant Proteins		
CL-316,243	Cayman Chemical	CAS 138908-40-4
Atglistatin	Cayman Chemical	CAS 1469924-27-3
L-Carnitine inner salt synthetic, ≥98%	Sigma-Aldrich	Cat# C0158
Palmitoyl-L-carnitine chloride ≥98% (TLC), powder	Sigma-Aldrich	Cat# P1645
Bovine Serum Albumin Fraction V, heat shock, fatty acid free	Sigma-Aldrich	Cat# 3117057001
Corn oil delivery vehicle for fat-soluble compounds	Sigma-Aldrich	Cat# C8267
Palmitoyl Carnitine Chloride, L-[Palmitoyl-1-14C]-, 10μCi (370kBq)	Perkin Elmer	Part# NEC667010UC
Chloroform	Millipore-Sigma	Cat# 1058-6
Methanol, ACS	VWR International	Cat# BDH1135-4LP
Urea reagent grade, 98%	Sigma-Aldrich	Cat# 208884
Sulfuric acid 99.999%	Sigma-Aldrich	Cat# 339741-500ML
Ultima Gold MV, 2x5L	Perkin Elmer	Part # 6013159
Fetal Bovine Serum	RBMI	Cat# FBS-BBT-5XM
Insulin, Recombinant Human	Sigma-Aldrich	Cat# 91077C-100MG
3,3′,5-Triiodo-L-thyronine sodium salt	Sigma-Aldrich	Cat# T6397-100MG
3-Isobutyl-1-methylxanthine (IBMX)	Sigma-Aldrich	Cat# I5879-1G
Dexamethasone	Sigma-Aldrich	D4902-100MG
Indomethacin	Sigma-Aldrich	Cat# I7378-10G
Rosiglitazone	Cayman Chemical	Cat# 71740
PALMITOYL-1,2,3,4-13C4-L-CARNITINE HCL, 99 ATOM % 13C Non Haz	Sigma-Aldrich (Isotec)	Material # 662127-CONF
HBSS	Thermo Fisher	Cat# 24020117
Collagenase from Clostridium histolyticum	Sigma-Aldrich	Cat# C6885-1G
Collagen, Type I solution from rat tail	Sigma-Aldrich	Cat# C3867-1VL
Trizol Reagent	Thermo Fisher	Cat# 15596018

(*Continued on next page*)

Continued

REAGENT or RESOURCE	SOURCE	IDENTIFIER
17:1 Lyso PC	Avanti Lipids	LM-1601; CAS 1246304-62-0
17:0-20:4 PE	Avanti Lipids	LM-1102; CAS 253127-52-5
17:0-20:4 PC	Avanti Lipids	LM-1002; CAS 214918-13-5
methyl tert-butyl ether	Mallinckrodt	5398-08; CAS 1634-04-4
Acetonitrile	Honeywell	LC-015-2.5; CAS 75-05-8
Isopropyl Alcohol	Honeywell	LC-323-4; CAS 67-63-0
formic acid	Sigma Aldrich	33015-500ML; CAS 607-001-00-0
Ammonium Formate	Alfa Aesar	14517; CAS 540-69-2
Methanol	Fisher	A452-4; CAS 67-56-1
d4-succinate internal standard	Sigma Aldrich	293075; CAS 14493-42-6
O-methoxylamine hydrochloride	MP Biomedicals	155405; CAS 593-56-6
pyridine	EMD Millipore	PX2012-7; CAS 110-86-1
N-methyl-N-trimethylsilyltrifluoracetamide (MSTFA)	Thermo	TS48915; CAS 24589-78-4
deuterium labled carnitine internal standards	Cambridge Isotope Laboratories	NSK-B-1; NSK- B-G1
fatty acid methyl ester standard (FAMES)	Supelco	CRM47885
Critical Commercial Assays		
Free Fatty Acid Quantitation Kit	Sigma-Aldrich	Cat# MAK044-1KT
LabAssay Triglyceride	Wako Chemicals	Cat# 290-63701
Primary Hepatocyte Maintenance Supplements	Thermo Fisher	Cat# CM4000
SS VILO MASTERMIX 500RXN 500 RXN	Thermo Fisher	Cat# 11755500
KAPA SYBR FAST ROX Low	Kappa Biosystems	Cat# KK4621
Liver In Vivo Transfection Kit	Altogen	Cat #5061
RIPA Buffer	Boston BioProducts	Cat# BP-115
Complete Protease Inhibitor Tablets - mini	Roche	Cat# 04693124001
Pierce BCA protein Assay Kit	Thermo Fisher	Cat# 23225
Laemmli Sample buffer	Bio-Rad	Cat# 161-0737
ChIP DNA Clean & Concentrator Kit	Genesee Scientific	Cat# 11-379
Experimental Models: Cell Lines		
Immortalized brown preadipocytes	This paper	Described in Rodriguez-Cuenca et al., 2007
primary hepatocytes	This paper	Described in Severgnini et al., 2012
Experimental Models: Organisms/Strains		
C57BL6J, male, 10 weeks old	Jackson Laboratories	Stock# 000664
B6.129X1(FVB)-Hnf4atm1.1Gonz/J	Jackson Laboratories	Stock# 004665
B6.Cg-Gt(ROSA)26Sortm9(CAG-tdTomato)Hze/J	Jackson Laboratories	Stock# 007909
B6N.129S-Pnpla2tm1Eek/J (AtgIFLOX)	Jackson Laboratories	Stock# 024278
B6;FVB-Tg(Adipoq-cre)1Evdr/J (Adipoq-Cre)	Jackson Laboratories	Stock# 010803
FVB/N-Tg(UcpDta)1Kz/J	Jackson Laboratories	Stock# 002384
Oligonucleotides		
DsiRNA - Cpt1b	IDT	Design ID mm.Ri.Cpt1b.13.1 from sequence NM_009948
DsiRNA - Cpt1a	IDT	Design ID mm.Ri.Cpt1a.13.1 from sequence NM_013495
Scrambled Negative Control DsiRNA	IDT	Cat# 51-01-19-09
RT-PCR Primers Table S1	This Paper	N/A
Software and Algorithms		
QuantStudio Software V1.3—for QuantStudio 6 and 7 Flex and ViiA 7 Real-Time PCR Systems	Thermo Fisher	https://www.thermofisher.com/us/en/home/technical-resources/software-downloads/quantstudio-flex-real-time-pcr-system.html

(*Continued on next page*)

Continued

REAGENT or RESOURCE	SOURCE	IDENTIFIER
Prism 7	GraphPad	https://www.graphpad.com/scientific-software/prism/
significance analysis of microarrays	Tusher et al., 2001	N/A
R version 3.1.3	this paper	https://cran.r-project.org/bin/windows/base/old/3.1.3/
Agilent Mass Hunter Qual B.05.00	Agilent	\\wscsfs01\LSCA\apgsup\Software\CURRENT\G3335AA MassHunter Quantitative Analysis Software B.05.00 Build 291.0\Service Packs\SP2
Agilent Mass Hunter Quant B.07.00	Agilent	http://www.agilent.com/en-us/support/software-informatics/quant-report-0700-sp1
MetaboAnalyst 3.0	Xia et al., 2015	http://www.metaboanalyst.ca
MassLynx 4.1 software	Waters	http://www.waters.com/waters/en_US/MassLynx-Mass-Spectrometry-Software-/nav.htm?cid=513164&locale=en_US

CONTACT FOR REAGENT AND RESOURCE SHARING

Further information and requests for resources and reagents should be directed to and will be fulfilled by the Lead Contact, Claudio Villanueva (villanueva@biochem.utah.edu).

EXPERIMENTAL MODEL AND SUBJECT DETAILS

Animal Care

All procedures were approved by the Institutional Animal Care and Use Committee (IACUC) of University of Utah. Mice were housed at 22°C–24°C using a 12 hr light/12 hr dark cycle. Animals were maintained on a Teklad global soy protein-free diet (2920x-030917M). Animals had ad libitum access to water at all times, and food was only withdrawn if required for an experiment. Male mice C57BL6J at 3-4 months of age, unless otherwise stated. Mice were purchased from Jackson Laboratories.

Genetic Mouse Models

C57BL6J male mice aged to 3 months were purchased from Jackson laboratories, older mice were provided by the National Institute on Aging. HNF4$\alpha^{F/F}$ mice were bred to C57BL/6 mice for five generations before crossing to homozygosity (Hayhurst et al., 2001). Male HNF4$\alpha^{F/F}$ mice were aged to 12 weeks, one week prior to cold exposure mice received intraperitoneal injection of adeno-associated virus 8 (AAV8) containing Cre recombinase regulated by the thyroid hormone binding globin promoter (AAV8-TBG-Cre) to drive hepatocyte specific expression or a control green fluorescent protein regulated by the same promoter (AAV8-TBG-eGFP) (University of Pennsylvania Vector Core in Philadelphia) (Hayashi et al., 1993; Mu et al., 2015). Mice received a single injection of 400μL of AAV8-TBG-eGFP or AAV8-TBG-Cre (titer 10^{12}genome copies/mL).

AAKO mice were generated from the previously described ATGL$^{F/F}$ mice which were bred with C57BL/6NJ mice for more than 10 generations (Haemmerle et al., 2011). ATGL$^{F/F}$ mice were then bred to Adipoq-Cre BAC transgenic mice bred for 9 generations by the Jackson laboratories to C57BL/6J background. The mice from this F1 generation were then crossed to generate ATGL$^{F/F}$ mice that expressed the Adipoq-Cre transgene and compared to littermate controls lacking cre transgene. For the procedures described in this manuscript, male AAKO mice and male litter mate controls ranging from 22 to 27 weeks of age were selected for an experimental cohort.

FVB/N-Tg(Ucp-DTA)1Kz/J mice expressing the diphtheria toxin A-chain using the UCP promoter containing 3 kb of 5'-flanking DNA and 0.3 kb of 3'-flanking DNA were acquired from the Jackson laboratory (Lowell et al., 1993). Male UCP-DTA mice were used for studies.

Brown Adipocyte

Brown preadipocytes were isolated from C57BL6J mice (Rodriguez-Cuenca et al., 2007). Interscapular BAT was removed from 4 week-old male C57BL6J mice in sterile conditions, minced into small pieces, and incubated in digestion buffer (0.1% collagenase type 2, DMEM, and antibiotic-50 IU Penicillan/mL and 50 μg Streptomycin/mL). The samples were incubated at 37°C in a shaking water bath for 1 hour. The solution was cooled at 4°C for 15-30 minutes, and then infranatant was filtered through a 100μm filter and centrifuged for 5 minutes at 700xg. The digestion buffer was removed and the pellet washed with DMEM and antibiotics (50 IU Penicillan/mL and 50 μg Streptomycin/mL), the cells were then centrifuged for 5 minutes at 700xg. The pellet was resuspended in 0.5 ml of DMEM with antibiotics, 0.2mL of this solution was added to a 6-well plate containing 1.8mL of cultured media (10% FBS, DMEM, and 50 IU Penicillan/mL and 50 μg Streptomycin/mL). The day after harvest, the cells were immortalized through retroviral

expression of SV40 Large T-antigen using hygromycin for selection (Rodriguez-Cuenca et al., 2007). For experiments, the cells were plated in DMEM containing 10% FBS (RMBI), 20nM insulin (Sigma), and 1nM T3 (Sigma). Upon complete confluence cells were stimulated for differentiation by DMEM containing 10% FBS, 20nM insulin, 1nM T3, 0.5mM isobutylmethylxanthine (Sigma), 0.5μM dexamethasone (Sigma), 0.125mM indomethacin (Sigma), and 1μM rosiglitazone (Cayman). After 2 days differentiation media was removed and cells were maintained in DMEM 10% FBS, 20nM insulin, 1nM T3, and 1μM Rosiglitazone. Validation of brown preadipocytes was performed by RT-PCR during a differentiation time course for BAT markers PPARγ2, UCP1, Eva1, Elov3, Ebf2 and Prdm16.

Primary Hepatocytes

Primary hepatocytes were isolated as previously described (Severgnini et al., 2012) from 8 week old male HNF4α$^{f/f}$ Rosa26LSL-tdTomato, a kind gift from the laboratory of Eric Snyder at the University of Utah. Briefly, animals were anaesthetized with 5% isoflurane, the animals were sacrificed by cervical dislocation, the abdominal cavity was opened, the rib cage removed while taking care not to rupture blood vessels, and the visceral vena cava exposed. A catheter of PE-10 tubing was inserted through the right atrium into the vena cava, the catheter was kept in place by applying a surgical knot with fibroin. The livers were perfused with sterile PBS back pressure was created during the perfusion process by clamping the inferior vena cava below the kidneys which had previously been severed for 5 second intervals. The liver was then perfused with DMEM with 0.15% Collagenase type II (Sigma) for 10 minutes, and then excised. The liver sac was then cut in sterile conditions in a 10cm dish in DMEM. The cells were passed through a 100μM cell strainer and then pelleted at 50 g for 1 minute, the pellet was washed 3 times with DMEM and then plated on a tissue culture plate coated with 0.1% rat tail collagen (Sigma). Cells were maintained in hepatic cell culture media (Thermo Fisher), and assessed for hepatocyte purity by RT-PCR of albumin, cyk18, and transthyretin.

METHOD DETAILS

Cold Exposure

Mice were singly housed with no food, no bedding, but ready access to water. Starting at T0 mice were placed at the specified temperature of either 30°C (thermoneutrality), 24°C (room temperature), 16°C, or 4°C (cold exposure) for 5 hours. Body temperatures were taken every hour with a physitemp A590 rectal probe using an Oaklon Thermocouple digital thermometer.

CL-316,243 Administration

Administration of CL-316,243 (1mg/kg body weight; Cayman) or a vehicle control of sterile PBS pH 7.5 was performed by intraperitoneal injection. After drug or vehicle administration mice were singly housed in a cage with no food, no bedding, but ready access to water placed at 24°C for 5 hours. After euthanasia tissues were dissected 5 hours after administration of CL-316,243 or saline, flash frozen in liquid nitrogen, and stored at -80°C.

Atglistatin Treatment

Atglistatin (200μmol/kg body weight; Caymen) was diluted in corn oil and provided by oral gavage, a comparable volume of corn oil was administered by gavage in the control mice (Mayer et al., 2013). For the duration of the cold exposure mice were singly housed in a cage with no food, no bedding, but ready access to water.

Carnitine and Palmitoylcarnitine Administration

Carnitine (100mg/kg body weight; Sigma) was administered by intraperitoneal injection with sterile PBS pH 7.5 used as a vehicle control. Palmitoylcarnitine (100μM; Sigma), palmitate conjugated to BSA (100μM; Sigma), or BSA solution was injected via tail vein. After administration of metabolites mice were placed at 4°C with no food, no bedding, but ready access to water.

Palmitate Treatment of Primary Hepatocytes

The day after primary hepatocytes isolation, cells were rinsed 8-10x to remove debris. Hepatocytes from HNF4α F/F mice were infected with adenovirus expressing either CMV-eGFP (GFP) or CMV-eGFP-Cre (CRE) (ViraQuest) at multiplicity of infection (MOI) of 1. 48 hours post infection cells were treated with indicated levels of BSA conjugated palmitate for 6 hours, washed 3 times with PBS, and then RNA was extracted.

Tissue Uptake of Palmitoylcarnitine

Mice received an intravenous injection through the tail vein using 120μL solution of 1μCi of ^{14}C-palmitoylcarnitine (PerkinElmer) mixed with unlabeled palmitoylcarnitine (Sigma) dissolved in sterile saline. The amount of unlabeled palmitoylcarnitine was adjusted to body weight, ensuring that the initial injection concentration was 10μM based on calculated blood volume (Riches et al., 1973). After injection, mice were placed in either Room Temperature (24°C) or Cold (4°C), body temperatures and blood samples were taken hourly. Mice were sacrificed after five hours, tissues were weighed and processed by Folch extraction (Pandey et al., 2012). Briefly, ~100mg of tissue was homogenized in 1.4mL chloroform/methanol (2:1) first by glass dounce followed by four cycles in the TissueLyzer II (Qiagen). Urea (40%) and sulfuric acid (5%) were added and the tubes were processed again by TissueLyzer II. Samples were centrifuged 1,800g for 10 minutes. The aqueous phase and organic phase were measured using liquid scintillation.

Brown Adipocyte ^{13}C-1,2,3,4-palmitoylcarnitine Labeling

On day 6 of differentiation brown adipocytes were washed 3 times with PBS, activated with 1μM CL-316,243, and then treated with 100μM ^{12}C-palmitoylcarnitine (Sigma) or 100μM ^{13}C-1,2,3,4-palmitoylcarnitine (Isotec) in Krebs Ringer Buffer (135mM NaCl, 5mM KCl, 1mM $MgSO_4$, .4mM K_2HPO_4, 5.5mM Glucose, 20mM HEPES, 1mM $CaCl_2$ pH 7.4). After 6 hours of palmitoylcarnitine treatment cells were washed 3 times with PBS and then collected using a cell scrapper for metabolic tracer analysis.

Hepatic Knockdown Studies

C57BL6J 3 month-old male mice received intravenous tail vein injection with 60μg of siRNA targeting Cpt1a, Cpt1b, both Cpt1a/Cpt1b, or scrambled negative control in a hepatocyte targeting liposome mixture (Altogen) (Bukong et al., 2014). Mice were injected a second time with 30ug of the specified siRNA liposome mixture twelve hours after the initial injection. Thirty-six hours after the initial injection, mice were singly housed without food but free access to water and placed at 4°C. A cold tolerance test was conducted as previously described; mice were sacrificed five hours after the start of cold exposure. The siRNAs were obtained from IDT using proprietary designs for the scrambled (51-01-19-09), Cpt1a (mm.Ri.Cpt1a.13.1), and Cpt1b (mm.Ri.Cpt1b.13.1).

Lipid Measurements

Lipids were extracted from serum (~40 μL) aliquots then combined with 225 μL ice-cold MeOH containing internal standards (Avanti Lipids, LM-1601 (19.82 μM, -1102 (14.52 μM) and -1002 (12.54 μM); 10 μL each / sample) and vortexed for 10 s. 750 μL of ice-cold MTBE (methyl tert-butyl ether) was added, vortexed for 10 s, and 200 μL of water is added to induce phase separation. The sample was then vortexed for 20 s followed by centrifugation at 14,000 g for 2 min at 4 °C. The upper phase (750 μL) was collected and evaporated to dryness under vacuum. Samples were reconstituted in 25 μL ACN:H_2O:IPA (1:1:2 *v/v*) + 0.1% formic acid for analysis. A pooled QC sample was prepared by 5 μL aliquots from each sample.

Lipid extracts were separated on an Acquity UPLC CSH C18 1.7 μm 2.1 x 100 mm column maintained at 60 °C connected to an Agilent HiP 1290 Sampler, Agilent 1290 Infinity pump, equipped with an Agilent 1290 Flex Cube and Agilent 6520 Accurate Mass Q-TOF dual ESI mass spectrometer. For positive more, the source gas temperature was set to 350 °C, with a gas flow of 11.1 (L/min) and a nebulizer pressure of 24 psig. VCap voltage is set at 5000 V, fragmentor at 250 V, skimmer at 74.4 V and Octopole RF peak at 750 V. VCap voltage is set at 5000 V, fragmentor at 100 V, skimmer at 75 V and Octopole RF peak at 750 V. Reference masses in positive mode (m/z 121.0509 and 922.0098) were infused with nebulizer pressure at 2 psig. Samples were analyzed in a randomized order acquiring with the scan range between m/z 100 – 1700. Mobile phase A consists of ACN:water (60:40 v/v) in 10 mM ammonium formate and 0.1% formic acid, and mobile phase B consists of IPA:water (90:10 v/v) in 10 mM ammonium formate and 0.1% formic acid. The chromatography gradient for both positive and negative modes starts at 15% mobile phase B increasing to 30% B over 4 min, it then increases to 52% B from 4-5 min, then increases to 82% B from 5-22 min, then increases to 95% B from 22-23 min, and then increases to 99% B from 23-27 min. From 27-38 min it's held at 99%B, then returned to 15% B from 38-38.2 min and was held there from 38.2-44 min. Flow is 0.3 mL/min throughout. Tandem mass spectrometry was conducted using the same LC gradient and at collision energies of 10 V, 20 V and 40 V. Injection volume was 3 μL.

Results from LC-MS experiments were collected using Agilent Mass Hunter Workstation and analyzed using the software package Agilent Mass Hunter Qual B.05.00. Using the Find By Formula (FBF) algorithm, MS/MS fragmentation and a Lipids PCLD database, possible assignments were generated then individually inspected. Compounds were also checked against the blank process sample to remove any artifacts. Once a list of confident assignments was made, a Mass Hunter Quant method was generated and the software program Mass Hunter Quant is used to analyze and integrate each compound. Lipids are normalized to LM-1601 response (PC(17:1(10Z)/0:0)). Representative chromatogram and corresponding standards can be found in Table S3. Serum free fatty acids were quantified by colorimetric kit according to the manufacturer's instruction (Sigma).

Acylcarnitine Analysis

Acylcarnitine analysis was performed according to a published procedure (Liu and Pasquali, 2005) (Figures 1E, S1A, and S1B). A Waters Acquity Ultra Performance LC solvent manager system was used for sample and mobile phase delivery. MS/MS analysis was performed on a Waters Quattro Premier XE tandem mass spectrometer operated in positive ion electrospray mode using MassLynx software. Acylcarnitines extracts were derivatised with butanolic HCl, dried, and resuspended in mobile phase for MS/MS analysis. Free carnitine and acetylcarnitine were monitored in selective reaction monitoring mode (SRM), while all other acylcarnitines were monitored using parent ion scan (*m/z* 85). A list of butylated acylcarnitine species are shown in Table S2. Acylcarnitines were quantified using stable isotope dilution method and NeoLynx software.

Metabolic Tracer Analysis

Brown adipose tissue was weighed in bead mill tubes containing 1.4 mm ceramic beads (Qiagen, Carlsbad, CA). Cold methanol containing *d*4-succinate as an internal standard was added to give a final methanol concentration of 80%. An Omni Bead Ruptor (Omni, Kennesaw, GA) was employed at 6.45 MHz for 30 seconds to disrupt the cells. The supernatant was transferred to fresh microfuge tubes and protein was precipitated by incubation at -20° C for 30 minutes. The extract was clarified by centrifugation at 20,000 x *g* followed by transfer to new fresh microfuge tubes and solvent removed en vacuo.

All GC-MS analysis was performed with a Waters GCT Premier mass spectrometer fitted with an Agilent 6890 gas chromatograph and a Gerstel MPS2 auto sampler. Dried samples were suspended in 40 μL of a 40 mg/mL O-methoxylamine hydrochloride (MOX) in

pyridine and incubated for one hour at 30° C. To auto sampler vials was added 25 μL of this solution. 40 μL of N-methyl-N-trimethylsilyltrifluoracetamide (MSTFA) was added automatically via the auto sampler and incubated for 60 minutes at 37° C with shaking. After incubation 3 μL of a fatty acid methyl ester standard (FAMES) solution was added via the auto sampler then 1 μL of the prepared sample was injected to the gas chromatograph inlet in the split mode with the inlet temperature held at 250° C. A 10:1 split ratio was used for analysis. The gas chromatograph had an initial temperature of 95° C for one minute followed by a 40° C/min ramp to 110° C and a hold time of 2 minutes. This was followed by a second 5° C/min ramp to 250° C, a third ramp to 350°C, then a final hold time of 3 minutes. A 30 m Phenomex ZB5-5 MSi column with a 5 m long guard column was employed for chromatographic separation. Helium was used as the carrier gas at 1 mL/min. Data was collected using MassLynx 4.1 software (Waters). Each isotope for the targeted metabolites were identified and their peak area was recorded using QuanLynx. All the extracted data was then corrected mathematically to account for natural abundance isotopes, and finally showed as the fraction of the total pool of citrate (Katajamaa and Orešič, 2005).

Gene Expression

RNA was isolated from liver, skeletal muscle, or BAT using Trizol reagent (Invitrogen), samples were homogenized with a TissueLyzer II (Qiagen). Reverse transcription was performed with SuperScript VILO Master Mix (Thermo Fisher). Quantification of gene expression was performed with KAPA SYBR FAST qPCR 2x Master Mix Rox Low (Kapabiosystems) on an Applied Biosystems QuantStuio 6 Flex Real-Time PCR System, 384-well. Analysis was performed by a calculated relative expression extrapolated from a standard curve for each primer pair that was then normalized to expression of the housekeeping gene RPL13. Primer pairs were designed with Universal Probe Library (Roche) or qPrimer Depot (https://mouseprimerdepot.nci.nih.gov/), a list of primer pairs is included in Table S1.

Protein Analysis

Liver tissue was homogenized by glass dounce in RIPA buffer (Boston Bioproducts) with added protease inhibitor (Roche). Tissue samples were spun at 12,000 x g for 10 minutes at 4°C and the supernatant was extracted. Protein quantification was performed by BCA assay (Thermo Fisher), diluted in Laemmli loading buffer (BioRad), heated at 70°C for 20 min, and run on a standard 10% acrylamide gel. Protein was transferred to Amersham Protran .45μM Nitrocellulose (GE healthcare) and blotted for Cpt1b (16331-1-AP, ProteinTech), Octn2 (16331-1-AP, ProteinTech), Apoa-IV (5700S, Cell Signaling), HNF4α (PP-H1415-00, R & D Systems), or β-Actin (3700S, Cell Signaling).

Chromatin Immunoprecipitation

Chromatin was prepared from snap frozen livers. Livers were minced in 1% formaldehyde in PBS and incubated for 10 minutes at room temperature. Followed by quenching with 125 mM glycine for 10 minutes at room temperature. Livers were then homogenized in TissueLyser II according to manufacturer's instructions. Samples were centrifuged at 400g for 5 min and resuspended in chip lysis buffer (25mM Tris pH8, 2mM EDTA, 150mM NaCl, 1% Triton X-100, 0.1% SDS) and sonicated in Diagenode pico bath sonicator for 33 cycles, 40 seconds on 40 seconds off. Chromatin was Immunoprecipitated with antibodies against IgG (PP64 EMD Millipore), HNF4α (PP-H1415-00, R & D Systems) overnight at 4°C in the presence of Dynabeads protein A (10001D, Invitrogen). DNA was purified with ChIP DNA Clean & Concentrator Kit (11-379, Genesee Scientific) and quantified by real-time PCR (ABI QuantStudio Flex6) using Syber green (KK4621, Kapa Biosystems). Occupancy was quantified using a standard curve and normalized to input DNA. Primers are listed in Table S1.

QUANTIFICATION AND STATISTICAL ANALYSIS

Assessment of lipidomics t-test p value, fold change, and generation of heat map were performed in MetaboAnalyst 3.0 (Xia et al., 2015). Comparison of the differentially abundant plasma lipids from 3 month old and 24 month old mice in Room Temperature or Cold was performed by significance analysis of microarrays (SAM) (Tusher et al., 2001). A tuning parameter, delta of 0.4, optimized the cutoff for significance with the estimation of false discovery rate (FDR) threshold q-value of 0.05. Volcano plot creation and SAM was performed using R (version 3.1.3). Comparison between two groups was completed by student T-test, while multiple comparisons were completed using Two-way ANOVA followed by a Tukey post-hoc analysis using Prism 7.